International Journal of Nanomedicine

Dovepress
open access to scientific and medical research

Open Access Full Text Article

ORIGINAL RESEARCH

Self-nanoemulsifying drug delivery system of bruceine D: a new approach for anti-ulcerative colitis

This article was published in the following Dove Press journal:
International Journal of Nanomedicine

Yao-Xing Dou,[1,2,*] Jiang-Tao Zhou,[3,4,*] Tong-Tong Wang,[2] Yan-Feng Huang,[1] Vicky Ping Chen,[5] You-Liang Xie,[1] Zhi-Xiu Lin,[6] Jian-Sheng Gao,[7] Zi-Ren Su,[1] Hui-Fang Zeng[2]

[1]Mathematical Engineering Academy of Chinese Medicine, Guangzhou University of Chinese Medicine, Guangzhou, People's Republic of China; [2]Department of Pharmacy, The First Affiliated Hospital of Chinese Medicine, Guangzhou University of Chinese Medicine, Guangzhou, People's Republic of China; [3]School of Pharmaceutical Sciences, Guangzhou University of Chinese Medicine, Guangzhou, People's Republic of China; [4]Shanxi Key Laboratory of Otorhinolaryngology Head and Neck Cancer, Shanxi Medical University, Taiyuan, People's Republic of China; [5]Department of Molecular Pharmacology and Experimental Therapeutics, Mayo Clinic, Rochester, MN, USA; [6]School of Chinese Medicine, Faculty of Medicine, The Chinese University of Hong Kong, Hong Kong, People's Republic of China; [7]Guangzhou Baiyunshan Mingxing Pharmaceutical Co. Ltd., Guangzhou, People's Republic of China

*These authors contributed equally to this work

Correspondence: Hui-Fang Zeng
Department of Pharmacy, The First Affiliated Hospital of Chinese Medicine, Guangzhou University of Chinese Medicine, No.16, Airport Road, Guangzhou, 510405, People's Republic of China
Tel/fax +86 20 3935 8213
Email gancaozhf@126.com

Background: Bruceine D (BD) is a major bioactive component isolated from the traditional Chinese medicinal plant *Brucea javanica* which has been widely utilized to treat dysentery (also known as ulcerative colitis [UC]).

Methods: To improve the water solubility and absolute bioavailability of BD, we developed a self-nanoemulsifying drug delivery system (SNEDDS) composing of MCT (oil), Solutol HS-15 (surfactant), propylene glycol (co-surfactant) and BD. The physicochemical properties and pharmacokinetics of BD-SNEDDS were characterized, and its anti-UC activity and potential mechanism were evaluated in TNBS-induced UC rat model.

Results: The prepared nanoemulsion has multiple beneficial aspects including small mean droplet size, low polydispersity index (PDI), high zeta potential (ZP) and excellent stability. Transmission electron microscopy showed that nanoemulsion droplets contained uniform shape and size of globules. Pharmacokinetic studies demonstrated that BD-SNEDDS exhibited enhanced pharmacokinetic parameters as compared with BD-suspension. Moreover, BD-SNEDDS significantly restored the colon length and body weight, reduced disease activity index (DAI) and colon pathology, decreased histological scores, diminished oxidative stress, and suppressed TLR4, MyD88, TRAF6, NF-κB p65 protein expressions in TNBS-induced UC rat model.

Conclusion: These results demonstrated that BD-SNEDDS exhibited highly improved oral bioavailability and advanced anti-UC efficacy. In conclusion, our current results provided a foundation for further research of BD-SNEDDS as a potential complementary therapeutic agent for UC treatment.

Keywords: bruceine D, self-nanoemulsifying drug delivery system, physicochemical properties, pharmacokinetics, anti-inflammation, anti-colitis activity

Introduction

Ulcerative colitis (UC) is a chronic inflammatory disorder of the gastrointestinal (GI) tract which is characterized by recurrent inflammatory involvement of colonic mucosa and submucosa. Physical signs of UC attack include bloody diarrhea, abdominal pain, constipation, abdominal distension, weight loss, fatigue, and vomiting.[1] The mechanism underling pathophysiological process of UC is complicated and the exact pathogenesis is not clear.[2,3] As the incidence of UC has increased rapidly over the past two decades, it has greatly affected the patients' quality of life.[4] To date, the principal drugs for UC are 5-aminosalicylic acid, immunosuppressive agents, antibiotics, and steroid hormones. Despite moderate therapeutic effects, these drugs have varying side effects that have greatly impeded their applications in clinical practice.[5] Therefore, there is an urgent need to identify effective alternatives for UC treatment.

submit your manuscript | www.dovepress.com
Dovepress
http://dx.doi.org/10.2147/IJN.S174146

UC is known as "changpi" in traditional Chinese medicine (TCM) with the symptoms of diarrhea, pus and blood stool, bellyache, and tenesmus.[6] *Brucea javanica (L.) Merr*, a family of *Simaroubaceae*, is a 10-feet tall shrub widely distributed in South China, Southeast Asia, and Northern Australia.[7] The desiccative ripe fruit of *B. javanica* (Ya-dan-zi in Chinese) is a famous traditional Chinese folk medicine commonly used to treat dysentery, malaria, hemorrhoids, corns, and other diseases.[8] Bruceine D (BD, $C_{20}H_{26}O_9$; the chemical structure is shown in Figure 1A) is a natural quassinoid isolated from *B. javanica* fruit.[9] BD has been reported to have various pharmacological activities including anti-pancreatic cancer,[10] anti-hepatocellular carcinoma,[11] human papillomavirus inhibitory effect, and so on.[12] Furthermore, BD exerts pronounced anti-inflammatory effects.[13] Our pilot experiments suggested that BD effectively attenuated colonic inflammation in rats. However, BD is a fat-soluble compound and barely dissolves in water making it difficult to disperse in aqueous solution. The low solubility creates a barrier for its absorption and release which results in poor bioavailability.[14] A new type of carrier for solving bioavailability and absorption problems is vital for the production of new medicines.[15] In recent years, the advanced nanotechnology has dramatically influenced drug delivery, especially in TCM. Nanonization technique not only effectively increases drug absorption, reduces dosage, and diminishes adverse reactions, but also has a significant role in the drug's sustained release and targeted therapy.[16]

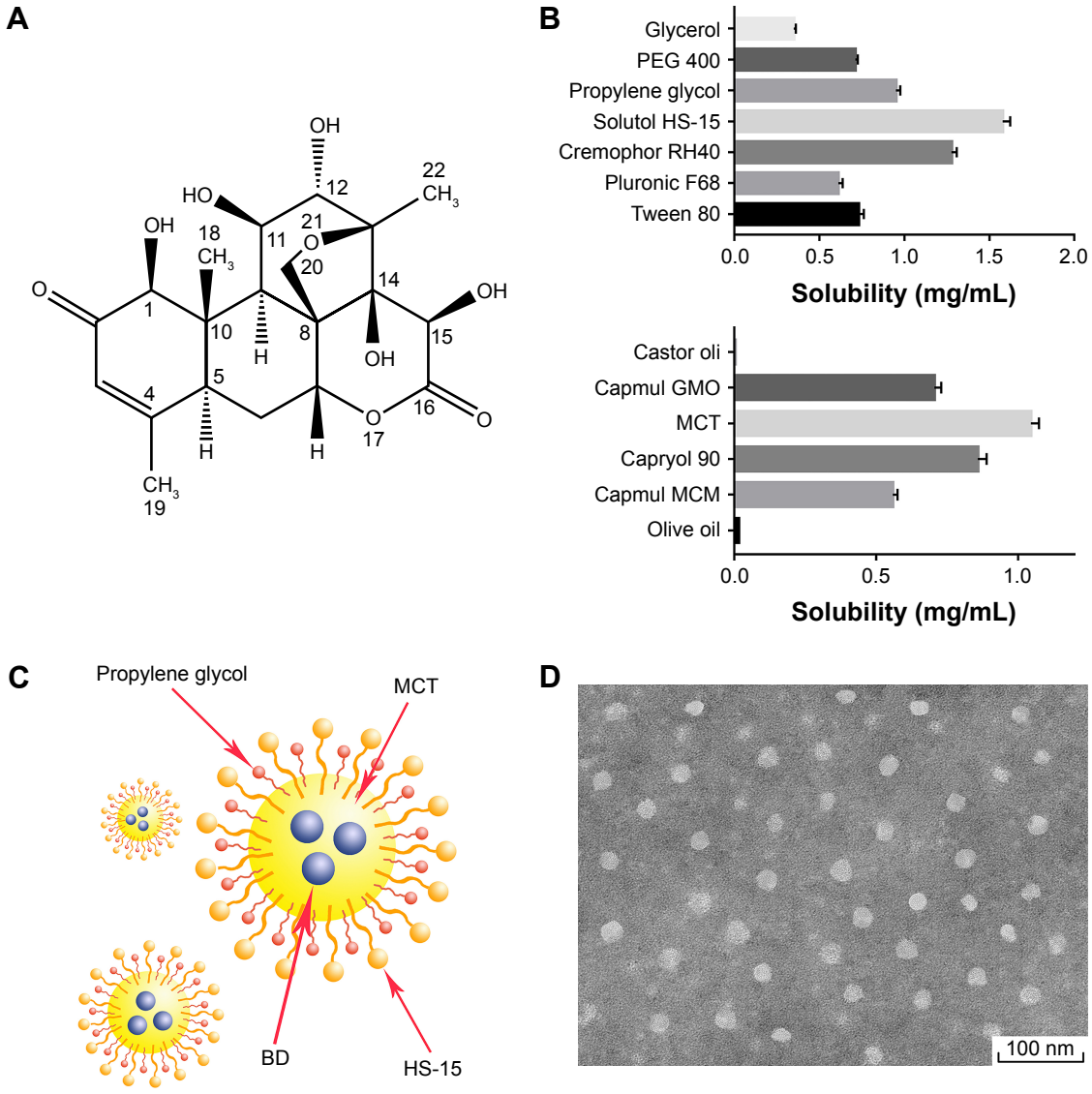

Figure 1 (**A**) Chemical structure of bruceine D. (**B**) Solubility of BD in different excipients. (**C**) The diagrammatic drawing of BD-SNEDDS. (**D**) TEM image of droplet BD-SNEDDS.

Abbreviations: BD, bruceine D; BD-SNEDDS, BD-loaded self-nanoemulsifying drug delivery system; MCT, medium-chain triglyceride; TEM, transmission electron microscopy.

Self-nanoemulsifying drug delivery system (SNEDDS) is an anhydrous formula of nanoemulsion, a homogenous liquid mix of surfactant(s), cosurfactant, oil, and drugs. When aqueous phase is added with mild stirring, O/W nanoemulsion is spontaneously formed. In vivo, the gentle peristalsis of GI tract provides the agitation for forming nanoemulsions.[17] SNEDDS can produce nanoemulsion droplets sized in the range of 20–200 nm under GI peristalsis.[18] Small globule size of SNEDDS provides a large interfacial surface area, which improves drug absorption and bioavailability by enhancing drug release and membrane permeation and reducing presystemic metabolism and efflux pump.[17]

The aim of the present study was to develop a formulation to enhance the solubility and bioavailability of BD. The optimized nanoemulsion formulation was obtained via ternary phase diagram. BD-SNEDDS was characterized by evaluating physicochemical properties of droplet size, polydispersity index (PDI), zeta potential (ZP), morphology, drug encapsulation efficiency, stability, and in vitro release test. Meanwhile, pharmacokinetics was investigated in parallel to the BD suspension. Furthermore, we tested the anti-UC activity and potential mechanism of BD-SNEDDS in rats with trinitrobenzenesulfonic acid (TNBS)-induced UC.

Materials and methods

Chemical and reagents

Kolliphor® HS-15 (PEG-15-hydroxystearate; BASF, Ludwigshafen, Germany), propylene glycol, and TNBS were obtained from Sigma-Aldrich (St Louis, MO, USA). MCT (C8) was purchased from Guangdong Mingkang Flavors & Fragrances Co., Ltd. (Guangzhou, Guangdong, People's Republic of China). Azathioprine (AZA) was from Aspen Pharmacare Australia Pty Ltd. (St Leonards, NSW, Australia). Pure water was supplied by A.S. Watson Group Ltd. (Hong Kong, People's Republic of China). All other ingredients, reagents, and solvents were of analytical grade.

BD was isolated from the fruit of the *B. javanica* (provided by Ming Xing Pharmaceutical Co. Ltd., Guangzhou, Guangdong, People's Republic of China). The structure of BD was elucidated by nuclear magnetic resonance (NMR).

Preparation of self-nanoemulsifying system and droplet size determination

Surfactant was dispersed in cosurfactant and then stirred (300 rpm, 25°C) with a magnetic stirrer for 30 minutes. Then, oil was added to the mixture, and stirred at 300 rpm for 30 minutes. After that, triplicate samples of various surfactants and oil compositions were diluted 100-fold with water, pre-equilibrated at 25°C, and gently mixed (300 rpm) by a magnetic stirrer, until homogeneous and clear.

The effects of different emulsifier structures, emulsifier concentrations, and oil structures on the nanoemulsion droplet size generated from SNEDDS were investigated. The droplet size and PDI were measured at 25°C by a Zetasizer Nano ZS (Malvern Instruments, Malvern, UK).

Solubility study

An equal amount of BD was added into stoppered glass penicillin bottles containing 1 mL of surfactant, cosurfactant or oil phase. Samples were sonicated for 10 minutes at 25°C and the mixtures were shaken for 24 hours at 37°C in water bath. After equilibrium for 2 hours at room temperature, the samples were centrifuged at 6,000 rpm for 10 minutes and the supernatants were diluted with methanol and filtered through a 0.45-μm millipore membrane for HPLC analysis.

Construction of pseudo-ternary phase diagrams

Different weight ratios (between 9:1 and 1:9) of surfactant and cosurfactant mixture (S_{mix}) to oil were tested to optimize the conditions of pseudo-ternary phase diagrams. To determine the region of nanoemulsions, S_{mix} and oil titrated with water were gently stirred by magnetic stirrers at 300 rpm until the mixture became transparent and slightly bluish. Analysis software OriginPro 9.1 (OriginLab Corporation, Northampton, MA, USA) was used to construct the pseudo-ternary phase diagrams. The experiment was performed in triplicate.

Preparation of BD-SNEDDS

BD-SNEDDS was prepared using HS-15, propylene glycol, and MCT at a weight ratio of 4:2:1 (w/w/w). BD was dissolved in MCT and then mixed with HS-15 and propylene glycol (PG) in a gentle magnetic stirring (300 rpm, 25°C, 30 minutes). After pre-equilibrium at room temperature, the solution was diluted 100-fold with double-distilled water and stirred till clear and slightly bluish.

Characterization of BD-SNEDDS

The droplet size, ZP, and PDI were measured at 25°C by a Zetasizer Nano ZS (Malvern Instruments) based on dynamic light scattering. The morphology of BD-SNEDDS was analyzed by Hitachi-HT7700 transmission electron microscope (Hitachi-Technologies Corp., Tokyo, Japan). Samples with a 500-fold dilution were placed on a copper grid (400 mesh). After the samples were dried, they were stained with phosphotungstic acid (2%) for 30 seconds prior to observation at room temperature.

Determination of entrapment efficiency (EE)

Freshly prepared SNEDDS (with a known amount of BD) was diluted with double-distilled water and centrifuged at 20,000 rpm for 2 hours at 4°C. The supernatant was collected and the free drug was quantified by HPLC (Shimadzu HPLC system, Kyoto, Japan). The EE was calculated according to the following equation:

$$EE\% = \frac{W_t - W_s}{W_t} \times 100$$

where EE represents the EE of BD-SNEDDS, W_t is the total BD quantity of sample, and W_s is the unentrapped BD in the supernatant. All these measurements were repeated three times.

Stability of BD-SNEDDS

The stability of BD-SNEDDS under extreme conditions including thermodynamic stability, gravitational stability, and pH stability was examined. BD-SNEDDS was diluted with deionized water with pH 1.2 and 6.8 (simulating gastric fluid and intestinal fluid, respectively). The samples were centrifuged at 6,000 and 12,000 rpm for 30 minutes to test the gravitational stability. The thermodynamic stability was evaluated by exposure in heating and cooling cycle from 20°C to −20°C for three times. Samples were also tested by heating at 50°C and cooling at 4°C for 30 minutes. The droplet size and ZP were measured after the above treatments.

In vitro release of BD-SNEDDS

The in vitro drug release assay of BD-SNEDDS was carried out on USP 24 dissolution test apparatus II.[19] In total, 5 mL of fresh BD-SNEDDS (containing 3 mg BD) or BD-suspension (3 mg BD suspended in 0.5% sodium carboxymethyl cellulose solution as control) was placed in a dialysis bag (molecular weight cut-off 8,000–14,000) surrounded by 500 mL of artificial gastric juice (0.1 M HCl, pH 1.2) or artificial intestinal juice (PBS pH 6.8). Then, the release medium was stirred at 100 rpm (37°C±0.5°C). At predetermined time points (0, 0.5, 1, 2, 4, 6, 8, 12, and 24 hours), 5 mL of sample solution was taken and replaced with the same volume of fresh release medium (37°C±0.5°C). After centrifugation at 10,000 rpm for 10 minutes, the supernatant was collected and analyzed by HPLC.

Pharmacological study

Male Sprague Dawley rats (200–220 g, n=12) were obtained from the Guangdong Medical Laboratory Animal Center (GDMLAC, Guangzhou, People's Republic of China). The Ethics Review Committee for Experimental Animal Center of Guangzhou University of Chinese Medicine approved the study (Permit ID: 2013–0020). All the experimental procedures were performed in accordance with the guidelines and regulations of Guangzhou University of Chinese Medicine. The animals were housed at controlled temperature of 22°C–24°C, humidity of 50%–60%, and 12-hour light/dark cycles. All rats were fasted for 12 hours with free access to water before experiments.

Twelve rats were randomly distributed into two groups, based on respective treatment at a dose of 3.0 mg/kg each: BD-SNEDDS and BD-suspension. The dosage was selected based on previous report[20] and our preliminary experiment.

Blood samples (0.25 mL each) were collected at 5, 15, 30, 45, 60, 90, 120, 240, 360, 480, 720, and 1,440 minutes from collecting blood from the rat eye socket veins after administration of respective doses. After centrifugation (3,000 rpm, 10 minutes), plasma was collected and stored at −20°C for further analysis. For deproteinization of plasma, ethyl acetate (200 µL) was added into the mixture and vortexed for 3 minutes. After centrifugation for 10 minutes (5,000 rpm), the supernatant was collected and vacuum dried at 40°C, −0.8 Mpa. The residue was redissolved with 100 µL methanol/water (v/v). After centrifugation (5,000 rpm, 10 minutes), the supernatant was analyzed by LC-MS/MS system.

Analysis software DAS (Version 3.0; Data Analysis System, Shanghai, People's Republic of China) was used to assess the pharmacokinetic parameters according to the non-compartmental model. With the concentration time curve ranging from 0 to 24 hours (AUC_{0-24}), the maximum plasma concentration (C_{max}), and peak time (T_{max}) were obtained directly from the plasma concentration vs time curve. The mean residence time (MRT_{0-24}), and the biological half-life time ($t_{1/2}$) were estimated from the terminal linear portion of the plasma concentration–time profile. The comparative *t*-test was applied by SPSS software to assess the statistical significance. All data are denoted as the mean±SD.

Anti-colitis activity of BD-SNEDDS

Experimental animals and colitis induction

Male Sprague Dawley rats (7 weeks; weighing 210–230 g) were supplied by Guangdong Medical Laboratory Animal Center. The animals were housed under a temperature-controlled environment (22°C–24°C), relative humidity (50%±10%), and 12:12 hours light–dark cycle with standard laboratory diet and water available ad libitum.

After acclimation for 1 week, animals were randomly divided into seven groups: Normal control (intact), TNBS group (vehicle), positive group (AZA), three doses of BD-SNEDDS groups (BDL-SNEDDS, BDM-SNEDDS, and BDH-SNEDDS; L-, M-, H- correspond to low-dosage, medium-dosage and high-dosage, respectively), and BD-suspension group (BD-suspended in 0.5% CMC-Na) (n=6). Before induction of colitis, all rats were fasted but with free access to clean water overnight to clean the bowel of animals. Briefly, animals were weighed and slightly anesthetized with pentobarbital sodium (25 mg/kg, i.p). TNBS solution was prepared by dissolving single dose of TNBS (25 mg/kg) in 50% alcohol (1 mL/kg of rat body weight). The TNBS solution was injected into the colon of rats through medical-grade rubber catheters inserted proximally 8 cm (from anus to colon). To prevent leakage of the instillation, rats were maintained in an upside-down position for 5 minutes after injection of TNBS. The intact group received 0.9% saline instead of TNBS solution. After installation, rats were recovered from anesthesia. During the experiment, body weight, feces characteristics, and activity were recorded every day for disease activity index (DAI) assessment.

Pharmacological treatment

After induction of colitis, drugs were administered by oral gavage for seven consecutive days. The intact group and TNBS group were given the same volume of blank SNEDDS. BD-SNEDDS group was given different doses of BD-SNEDDS (0.75, 1.5, and 3.0 mg/kg). The selection of BD dosage was based on the previous literature[21] and our pre-experiment. BD-suspension group was given BD suspension (3.0 mg/kg). Positive group received AZA (9.0 mg/kg) according to a previous report.[22] Animals were sacrificed on the eighth day of the experiment.

Evaluation of colonic damage

According to the standard scoring system, weight changes, diarrhea, and hematochezia were evaluated every day by an investigator blinded to the experimental protocol. DAI was determined as Sun et al previously described.[23] DAI was calculated according to the weight loss, stool consistency, and bleeding. On day 8, following induction with TNBS, animals were sacrificed under anesthetized condition by pentobarbital sodium. Colorectums were removed and the length was measured. The macroscopically visible damage on the colon was assessed by two observers unaware of the treatments according to a reported scoring system.[24] Scoring rules were as follows: 0, normal; 1, localized hyperemia, no ulcers; 2, ulceration without hyperemia or bowel wall thickening; 3, ulceration with inflammation at one site; 4, two or more sites of ulceration and inflammation; 5, major sites of damage extending >1 cm along the length of the colon; and 6–10, if major sites of damage extending >2 cm along the length of the colon, the score is increased by one for each additional centimeter of involvement.

Histologic assessment of colons

Colons were cut into small segments, fixed in 4% paraformaldehyde, embedded in paraffin, and stained with hematoxylin and eosin (H&E). Histological evaluation was performed under a light microscope (Olympus DP73, Tokyo, Japan). Histological scores were blindly evaluated by two pathologists in accordance with the standard described previously.[25]

Assessment of tissue cytokine levels

The concentrations of pro-inflammatory cytokines (tumor necrosis factor-α [TNF-α], interleukin-1β [IL-1β], IL-6, and IL-8) and anti-inflammatory cytokines (transforming growth factor-β [TGF-β] and IL-10) in the colorectal tissues were detected by ELISA kits (CUSABIO Biotech Co., Ltd, Wuhan, People's Republic of China) according to the corresponding manufacturer's instructions. Colon tissues were homogenized in PBS and the levels of superoxide dismutase (SOD), malondialdehyde (MDA), myeloperoxidase (MPO), glutathione peroxidase (GSH-Px), and reactive oxygen species (ROS) were measured by assay kits (Jiancheng Company, Nanjing, China). The total protein concentrations were determined by bicinchoninic acid (BCA) protein assay kit (Jiancheng Company, Nanjing, China). The absorbance was measured using a multimode microplate reader (Multiskan GO 1510, Thermo Fisher Scientific, Waltham, MA USA).

Immunohistochemistry analysis

Formalin-fixed, paraffin-embedded colorectal tissues were sectioned into slices (thickness, 4 μm). The paraffin sections were dewaxed, rehydrated, and incubated with anti-NF-κB p65 (Abcam, Cambridge, UK) antibody at 4°C overnight. Sections were then incubated with corresponding goat anti-rabbit secondary antibody and labeled with horseradish peroxidase (37°C, 30 minutes). After wash, the slides were stained with 3,3′-diaminobenzidine (DAB) followed by re-dyeing with hematoxylin. Finally, the sections were photographed under a DP73 light microscope. The integrated optical density of each section was calculated by Image-Pro Plus 6.0 software (Media Cybernetics, Inc., Rockville, WA, USA).

Determination of *iNOS* and *COX*-2 mRNA expression by qRT-PCR

Total tissue RNAs was extracted using TRIzol™ (Thermo Fisher Scientific, Waltham, MA, USA) and processed with RevertAid First Strand cDNA Synthesis Kit (Thermo Fisher Scientific) per the manufacturer's instructions. Real-time PCR was performed with FastStart Universal SYBR Green Master (Rox; Roche, Basel, Switzerland). Primer sequences are listed in Table 1.

Western blot analysis

Colorectal tissues were homogenized using RIPA buffer with Protease Inhibitor Cocktail (1:100). Supernatants were collected after centrifugation. Protein content was determined by BCA protein assay kit (Cell Signaling Technology, Danvers, MA, USA). Equal volume of proteins was loaded onto SDS-PAGE gels and electrophoretically transferred onto polyvinylidene difluoride membranes. Subsequently, membranes were blocked with 5% skimmed milk in TBST (20 mM Tris/HCl pH 7.2, 150 mM NaCl, and 0.1% Tween 20) at room temperature for 1 hour. After incubation at 4°C overnight with the corresponding primary antibodies against TLR4, MyD88, TRAF6, and NF-κB p65, and β-actin (internal control) (Abcam, Cambridge, UK), the membranes were then incubated with secondary antibodies for 2 hours at room temperature. Finally, the membranes were treated with an enhanced chemiluminescence (ECL) reagent (Thermo Fisher Scientific, USA). The immunoreactive proteins were detected by ECL Western blot system (Tanon 4200 SF; Tanon Science & Technology, Shanghai, China). Protein bands were quantified by the software Quantity One (Version 4.6.2; Bio-Rad Corporation, Hercules, CA, USA).

Data analysis

The experimental data were expressed as mean±SD and analyzed with statistical analysis software SPSS (Statistical Product and Service Solutions, Version 23.0; IBM Corporation, Armonk, NY, USA). To analyze the statistical differences among groups, one-way ANOVA was applied. To determine the statistical significance, Dunnett's significant post hoc test was used. Statistical significance was set at $P<0.05$.

Table 1 Primer sequences

Targeted gene	Direction and sequence
iNOS	Forward: CTCAGCAGCATCCACGCCAAG
	Reverse: AGAACAATCCACAACTCGCTCCAAG
COX-2	Forward: TTCTCCAACCTCTCCTACTACACCAG
	Reverse: ATACACCTCTCCACCGATGACCTG
GAPDH	Forward: ACAGCAACAGGGTGGTGGAC
	Reverse: TTTGAGGGTGCAGCGAACTT

Abbreviations: *iNOS*, inducible nitric oxide synthase; *COX-2*, cyclooxygenase-2; *GAPDH*, glyceraldehyde-3-phosphate dehydrogenase.

Results

Structure elucidation of BD

^{1}H NMR (400 MHz, DMSO-d_6) δ ppm: 5.25 (1H, s, H-1), 5.98 (1H, s, H-3), 2.89 (1H, d, *J*=13.5 Hz, H-5), 2.14 (1H, d, *J*=14.6 Hz, H-6α), 1.68 (1H, m, H-6β), 5.12 (1H, s, H-7), 2.32 (1H, d, *J*=4.5 Hz, H-9), 4.96 (1H, s, H-11), 4.26 (1H, m, H-12), 3.53 (1H, d, *J*=4.2 Hz, H-14), 3.60 (1H, d, *J*=6.7 Hz, H-15), 1.25 (3H, s, H-18), 1.89 (3H, s, H-19), 3.64 (1H, m, H-20a), 4.91 (1H, s, H-20b), 1.04 (3H, s, H-22), 5.35 (1H, s, 1-OH), 4.38 (1H, d, *J*=3.5 Hz, 11-OH), 4.30 (1H, d, *J*=6.8 Hz, 12-OH), 5.34 (1H, s, 15-OH), ^{13}C NMR (100 MHz, DMSO-d_6) δ ppm: 81.4 (C-1), 198.3 (C-2), 124.0 (C-3), 163.4 (C-4), 48.7 (C-5), 27.1 (C-6), 80.8 (C-7), 47.6 (C-8), 42.3 (C-9), 43.7 (C-10), 73.7 (C-11), 79.8 (C-12), 83.1 (C-13), 78.6 (C-14), 69.0 (C-15), 173.7 (C-16), 22.1 (C-18), 10.9 (C-19), 68.5 (C-20), 18.3 (C-22). By comparing its NMR with the published data,[26] this compound was confirmed to be bruceine D (the NMR spectra of BD is shown in Figures S1 and S2).

Effects of emulsifier structure on the nanoemulsion droplet size generated from SNEDDS

Effects of different emulsifiers on droplet size were measured (Table 2). The results showed that HS-15 (POE stearate, hydrophilic–lipophilic balance (HLB) value ranging 12–14) had the smallest droplet size and PDI compared with Cremophor RH 40 (POE castor oil, HLB value ranging

Table 2 Effects of emulsifier structures on droplet size

Surfactant	DS (nm)	PDI
Cremophor RH 40 (HLB=14–16)	48.42±0.79	0.182±0.0214
HS-15 (HLB=12–14)	18.13±0.34	0.047±0.0051
Pluronic F68 (HLB=29)	71.97±1.76	0.265±0.0660
Tween 80 (HLB=15)	94.91±2.17	0.445±0.0512

Notes: MCT and propylene glycol as oil and cosurfactant, respectively. Surfactant, cosurfactant, and oil at a weight ratio of 4:2:1 (w/w/w). Data are expressed as mean±SD (n=3).

Abbreviations: DS, droplet size; PDI, polydispersity index; HLB, hydrophilic–lipophilic balance; Cremophor RH40, a polyoxyl 40 hydrogenated castor oil; HS-15, PEG-15-hydroxystearate; Pluronic F68, poloxamer 188; Tween 80, polysorbate 80; MCT, medium-chain triglyceride.

Table 3 Effects of emulsifier concentrations on droplet size

Km ratio	DS (nm)	PDI index
1:4	68.35±0.76	0.067±0.0065
1:3	56.21±0.87	0.056±0.0042
1:2	44.19±0.52	0.053±0.0075
1:1	32.82±0.42	0.051±0.0065
2:1	18.33±0.28	0.047±0.0045
3:1	17.62±0.44	0.042±0.0031
4:1	16.21±0.12	0.042±0.0050

Notes: HS-15, MCT, and propylene glycol as surfactant, oil, and cosurfactant, respectively. S_{mix} and oil at a weight ratio of 6:1 (w/w). Data are expressed as mean±SD (n=3).
Abbreviations: DS, droplet size; PDI, polydispersity index; Km ratio, the ratio of surfactant to cosurfactant; HS-15, PEG-15-hydroxystearate; MCT, medium-chain triglyceride.

14–16), Pluronic F68 (poly(ethylene oxide)–poly(propylene oxide)–poly(ethylene oxide)-triblock copolymers, HLB value of 29), and Tween 80 (polysorbates, average HLB value of 15).

Effects of emulsifier concentration and oil structure on the droplet size

In the present study, we investigated the effects of different emulsifier concentrations on droplet size. As shown in Table 3, different ratios of S_{mix} (1:4, 1:3, 1:2, 1:1, 2:1, 3:1, and 4:1 for HS-15:propylene glycol) displayed different droplet size distributions. The S_{mix} ratio of 2:1 resulted in small droplet size and PDI, and no significant change of droplet size was observed when the ratio of S_{mix} was greater than 2:1.

In addition, we also explored the effects of different types of oil on droplet size. The result obtained showed that castor oil and olive oil (fatty oil) could not form SNEDDS. When compared with Capryol-90 (PG fatty acid esters), Capmul-GMO (long-chain mono-glycerides), and Capmul-MCM (medium-chain mono-diglycerides), MCT exhibited the smallest droplet size and PDI (Table 4). Herewith, MCT was employed as the oil phase in preparing BD-SNEDDS.

Table 4 Effects of different oil structures on droplet size

Oil	DS (nm)	PDI
Capmul-GMO	122.99±1.65	0.245±0.0255
Capmul-MCM	44.95±0.39	0.179±0.0172
MCT	18.22±0.23	0.047±0.0080
Capryol-90	31.71±0.43	0.145±0.0129

Notes: HS-15 and propylene glycol as surfactant and cosurfactant, respectively. Surfactant, cosurfactant and oil at a weight ratio of 4:2:1 (w/w/w). Data are expressed as mean±SD (n=3).
Abbreviations: DS, droplet size; PDI, polydispersity index; GMO, long-chain mono-glycerides; MCM, medium-chain mono-diglycerides; MCT, medium-chain triglyceride.

Solubility study

In order to select the best excipient for BD-SNEDDS system, the solubility of BD in different solvent media was evaluated, as shown in Figure 1B. The best surfactant containing maximum solubility of BD was HS-15 (1.578 mg/mL), a commonly used solubilizing and emulsifying agent.[27–29] Propylene glycol and MCT (0.950 and 1.045 mg/mL, respectively) displayed the highest solubilizing capacity among cosurfactants and oil phases. Propylene glycol (propane-1,2-diol) is a common organic solvent and drug excipient. MCTs are often used to prepare nano- and micro-particulate formulations.[30–32] Therefore, HS-15, propylene glycol, and MCT were selected as the surfactant, cosurfactant, and oil, respectively.

Construction of pseudo-ternary phase diagrams

Pseudo-ternary phase diagrams were constructed in the absence of BD to identify the self-emulsifying region and to optimize the proportion of SNEDDS formulations. Based on the results of solubility studies, HS-15 (surfactant), propylene glycol (cosurfactant), and MCT (oil) were applied to construct the pseudo-ternary phase diagrams. As shown in Figure 2, different ratios of S_{mix} (1:1, 2:1, 3:1, and 4:1 for HS-15:propylene glycol) had different nanoemulsion areas (Figure 2). Notably, SNEDDS had the largest region with the S_{mix} ratio of 2:1. Therefore, the optimum ratio of S_{mix} was determined as 2:1.

Characterization of BD-SNEDDS

At the optimum formulation, BD-SNEDDS had a mean droplet size of 18.03±0.59 nm, ZP of −15.76±0.42 mV, and PDI of 0.045±0.0098, respectively (Figure 3). Transmission electron microscopy (TEM) images indicated that BD-SNEDDS exhibited homogeneous and spherical globules with small droplet size of less than 100 nm (Figure 1D). The EE of BD-SNEDDS determined by ultracentrifugation was 84.2%±1.5%. According to the definition of SNEDDS and the characterizations of BD-SNEDDS, a diagram of BD-SNEDDS is displayed in Figure 1C.

Stability of BD-SNEDDS

After centrifugation, heating, cooling, and freeze–thaw cycles, the formulation was still homogeneous and all the indexes had no significant difference ($P>0.05$; Table 5). In addition, dilutions with different pHs had no obvious effect on BD-SNEDDS ($P>0.05$; Table 5).

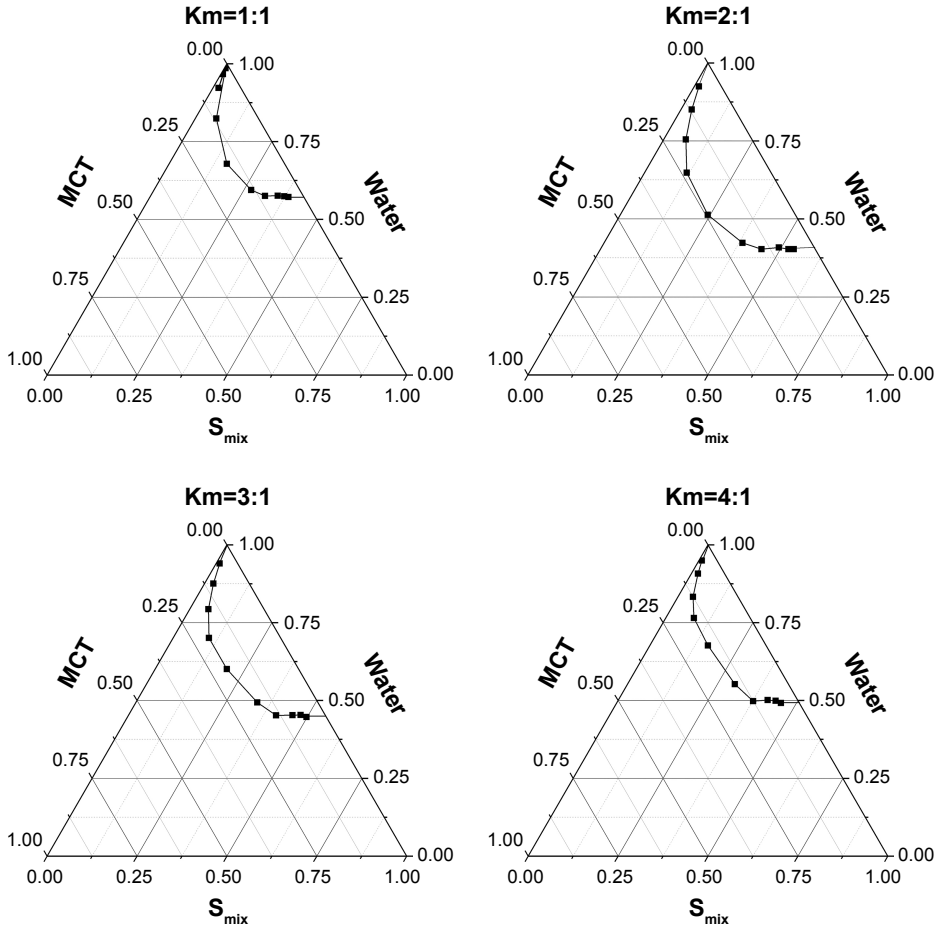

Figure 2 Pseudo-ternary phase diagrams of blank SNEDDS in K_m value of 1:1, 2:1, 3:1, and 4:1.
Abbreviations: K_m, the ratio of surfactant to cosurfactant; MCT, medium-chain triglyceride; SNEDDS, self-nanoemulsifying drug delivery system; S_{mix}, the mixture of surfactant and cosurfactant.

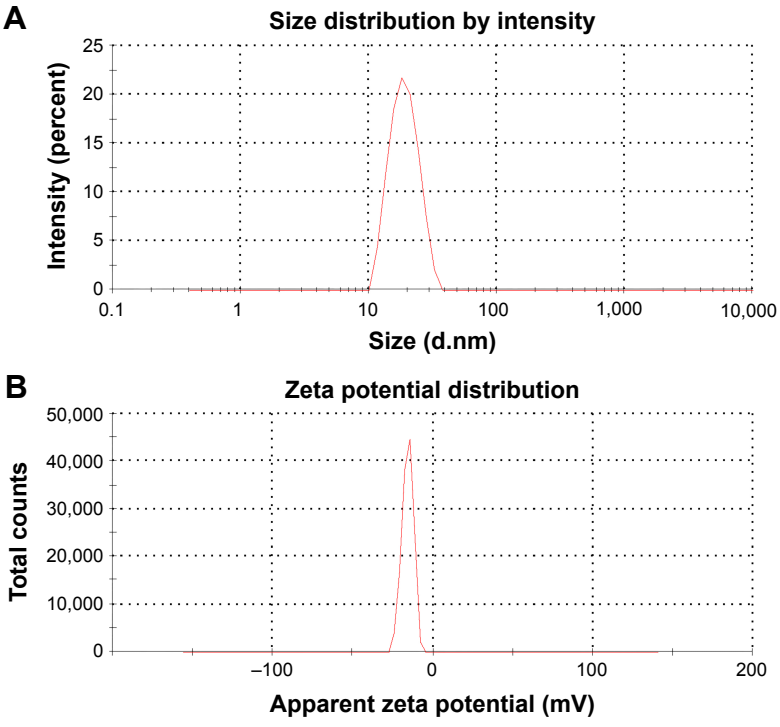

Figure 3 (**A**) Droplet size and distribution of BD-SNEDDS. (**B**) Zeta potential of BD-SNEDDS.
Abbreviation: BD-SNEDDS, BD-loaded self-nanoemulsifying drug delivery system.

Table 5 Effects of centrifugation, heating, cooling, and freeze–thaw cycles and aqueous phase pH on droplet size, polydispersity index, and zeta potential of BD-SNEDDS

Treatment	DS (nm)	ZP (mV)	PDI
No treatment	18.03±0.59	−15.76±0.42	0.045±0.0098
6,000 rpm, 30 minutes	18.79±0.52	−15.56±0.70	0.047±0.0078
12,000 rpm, 30 minutes	18.75±0.47	−15.48±0.26	0.039±0.0025
50°C, 30 minutes	18.82±0.33	−15.16±0.24	0.044±0.0062
4°C, 30 minutes	18.69±0.30	−15.63±0.35	0.042±0.0095
Freezing and thawing (−20°C, 20°C)	18.60±0.51	−14.90±0.88	0.042±0.0072
pH 1.2	18.64±0.42	−15.77±0.45	0.039±0.0089
pH 6.8	18.60±0.32	−15.93±0.32	0.039±0.0072

Note: Data are expressed as mean±SD (n=3).
Abbreviations: DS, droplet size; PDI, polydispersity index; ZP, zeta potential; BD-SNEDDS, BD-loaded self-nanoemulsifying drug delivery system.

Drug release

The release of BD from BD-SNEDDS was evaluated in simulated intestinal fluid (pH 6.8) and gastric fluid (pH 1.2), respectively. As illustrated in Figure 4B, the accumulative release percentage of BD from SNEDDS in simulated intestinal fluid (pH 6.8) was significantly greater than that in simulated gastric fluid (pH 1.2). Meanwhile, BD-suspension exhibited similar release efficiency. In both release media, the release rate of BD-SNEDDS was far more than that of BD-suspension. The accumulative release of BD-SNEDDS was 86.35% in phosphate buffer (pH 6.8) and 42.41% in HCl (pH 1.2) within 24 hours, while BD-suspension was 25.37% and 20.59%, respectively.

Pharmacokinetic behavior

The pharmacokinetic study was performed to quantify the amount of BD in SNEDDS or suspension through oral administration (3 mg/kg) in rats (Figure 4A). The result showed a significantly higher plasma drug concentration in BD-SNEDDS-treated rats compared with BD-suspension treated control. The C_{max} of BD-SNEDDS was found to be considerably higher than that of BD-suspension ($P<0.05$). In particular, T_{max} was shorter and AUC_{0-24h} was larger in BD-SNEDDS group than that of BD-suspension group ($P<0.05$; Table 6).

Anti-colitis activity of BD-SNEDDS

BD-SNEDDS reduces macroscopic damage

The body weight of all experimental groups had no significant difference at the beginning of the experiment. During the experiment, there was a noticeable body weight loss in rats treated with TNBS compared with control group which had a continuous weight gain. However, the body weight loss was significantly attenuated in BD-SNEDDS groups and AZA group (Figure 5C).

On the following day of TNBS induction, rats exhibited significant watery stool and bleeding till the termination of the study. Oral administration of BD-SNEDDS significantly alleviated diarrhea and bloody stool in a dose-dependent manner. As a common parameter for evaluating the severity of colonic inflammation, a higher DAI score indicates more severe colitis damage. After TNBS induction, the score of DAI increased rapidly compared with the normal group ($P<0.01$). However, the DAI scores of BD-SNEDDS groups were significantly lower in a dose-dependent manner ($P<0.01$). The BD-suspension group showed no statistically significant difference compared with BDM-SNEDDS group and positive control ($P>0.05$). Nevertheless, the score of BDH-SNEDDS group

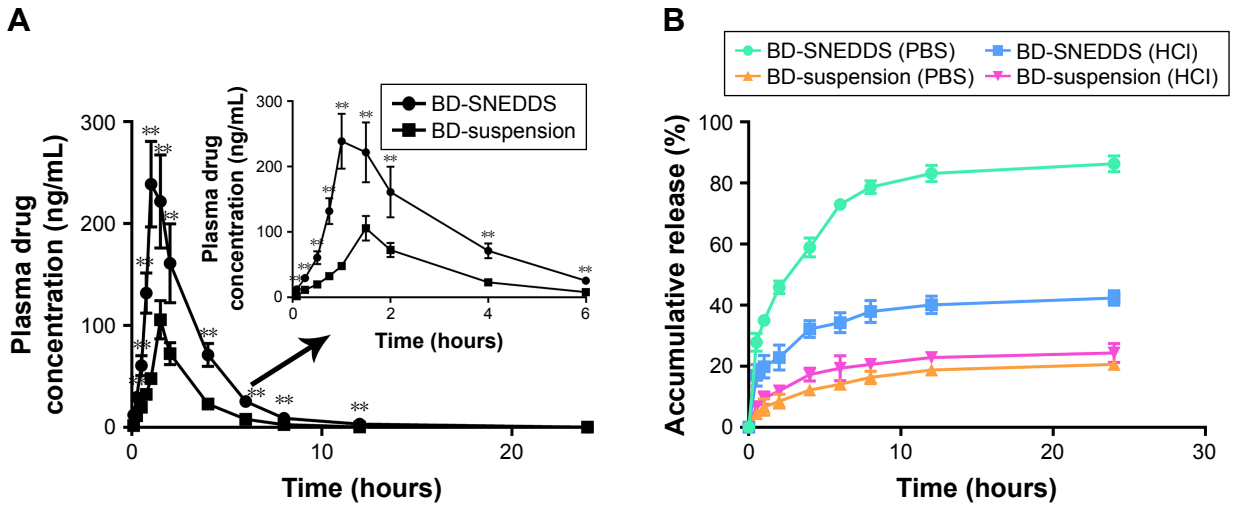

Figure 4 (**A**) Plasma concentration–time profiles of rats after oral administration of BD-SNEDDS and BD-suspension. (**B**) The in vitro release of BD-SNEDDS and BD-suspension in artificial intestinal juice (PBS, pH=6.8) and artificial gastric juice (HCl, pH=1.2).
Notes: Data are expressed as mean±SD (n=6). **$P<0.01$ vs suspension group.
Abbreviations: BD-SNEDDS, BD-loaded self-nanoemulsifying drug delivery system; BD-suspension, BD suspended in 0.5% sodium carboxymethyl cellulose solution.

Table 6 Pharmacokinetic parameters of BD after oral administration of BD-SNEDDS and BD-suspension

Parameter	BD-SNEDDS	BD-suspension
C_{max} (ng·mL^{-1})	258.34±34.68	108.36±13.75
T_{max} (hour)	1.08±0.20	1.58±0.20
$t_{1/2}$ (hour)	2.59±0.13	1.49±0.04
AUC_{0-24} (ng·hour·mL^{-1})	703.51±93.51	251.34±14.93
MRT_{0-24} (hour)	3.00±0.17	2.79±0.08
Relative bioavailability (%)	280.0	

Note: Data are expressed as mean±SD (n=6).
Abbreviations: BD-SNEDDS, BD-loaded self-nanoemulsifying drug delivery system; BD-suspension, BD suspended in 0.5% sodium carboxymethyl cellulose solution as control; C_{max}, maximum plasma concentration; T_{max}, time to reach the maximum plasma drug concentration; $t_{1/2}$, half-life elimination time; AUC_{0-24}, area under the plasma drug concentration–time curve ranging from 0 to 24 hours; MRT_{0-24}, mean residence time.

(3 mg/mL) was significantly lower than that of BD-suspension group (3 mg/mL; $P<0.01$; Figure 6A).

Colon length is another important index to reflect the severity of TNBS-induced colitis. Compared with the normal group, TNBS group showed a significant decrease of colonic length ($P<0.01$), whereas the shortening of colon length was significantly prevented by the BDM-SNEDDS and BDH-SNEDDS treatments ($P<0.01$; Figure 5B).

BD-SNEDDS treatments effectively ameliorated the colon mucosal damage in TNBS-treated rats, including edema, hyperemia, bowel wall thickening, mucosal erosions, and ulcers (Figure 7). The macroscopic score of colonic damage was 5.08±0.95 in TNBS group and reduced to 1.92±0.64 with AZA, 3.42±0.76 with BD-suspension, 4.58±0.86 with BDL-SNEDDS, 2.92±0.86 with BDM-SNEDDS, and 2.08±0.78 with BDH-SNEDDS (all $P<0.01$ vs TNBS group).

Effects of BD-SNEDDS on histological alternation

As demonstrated in Figure 5A, colon tissues from the control group exhibited intact mucosa, submucosa, smooth muscular layer, and outer membrane. TNBS group exhibited a number of inflammatory features, including inflammatory cells infiltration in the mucosa and lamina propria, distortion or

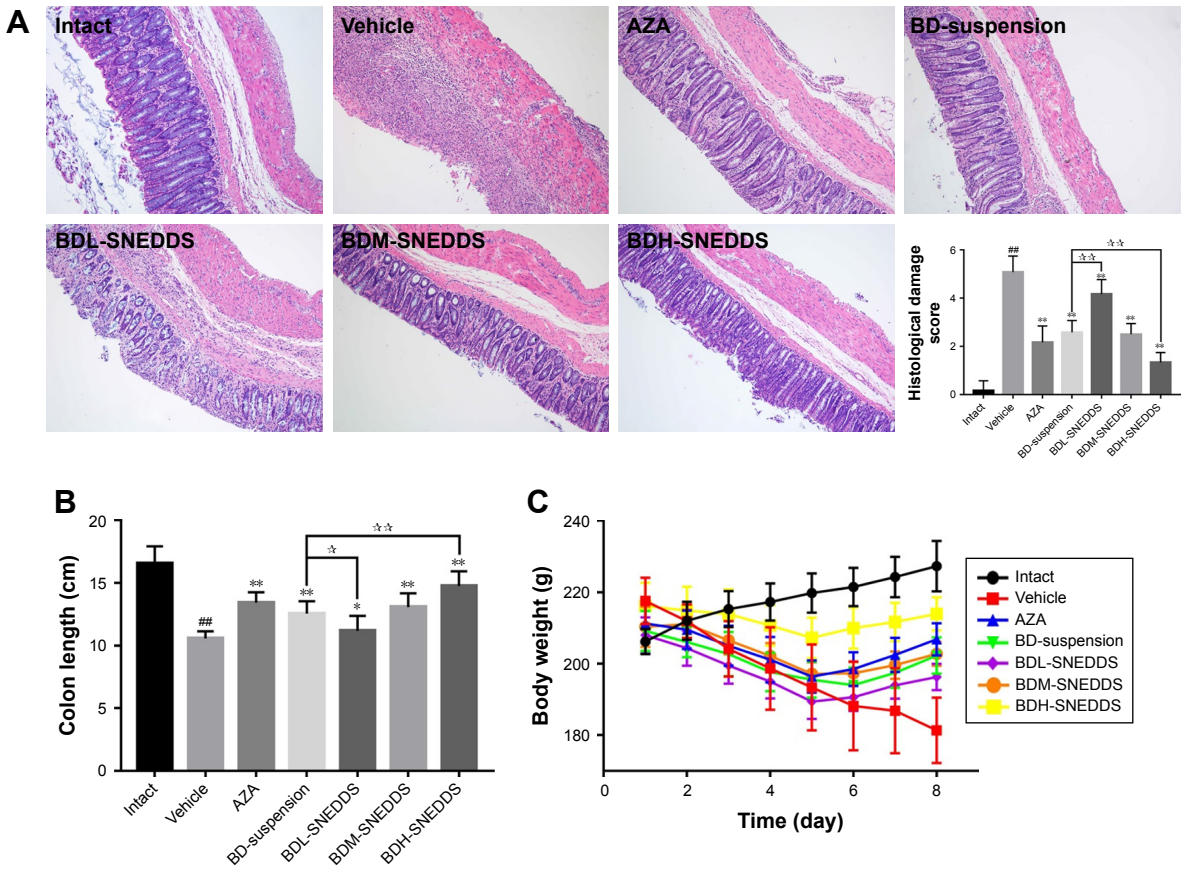

Figure 5 (**A**) Effects of BD-SNEDDS on histological changes (H&E staining slices from colorectal sections; original magnification 100×) and corresponding histological damage score. (**B**) The colon lengths. (**C**) Effects of BD-SNEDDS on body weight change.
Notes: Data are presented as mean±SD (n=6). ##$P<0.01$ vs intact group, *$P<0.05$ and **$P<0.01$ vs vehicle group, ☆$P<0.05$ and ☆☆$P<0.01$ vs BD-suspension group.
Abbreviations: BD-SNEDDS, BD-loaded self-nanoemulsifying drug delivery system; BD-suspension, BD suspended in 0.5% sodium carboxymethyl cellulose solution; H&E, hematoxylin-eosin; AZA, azathioprine; BDL-SNEDDS, low-dosage BD-loaded self-nanoemulsifying drug delivery system; BDM-SNEDDS, medium-dosage BD-loaded self-nanoemulsifying drug delivery system; BDH-SNEDDS, high-dosage BD-loaded self-nanoemulsifying drug delivery system.

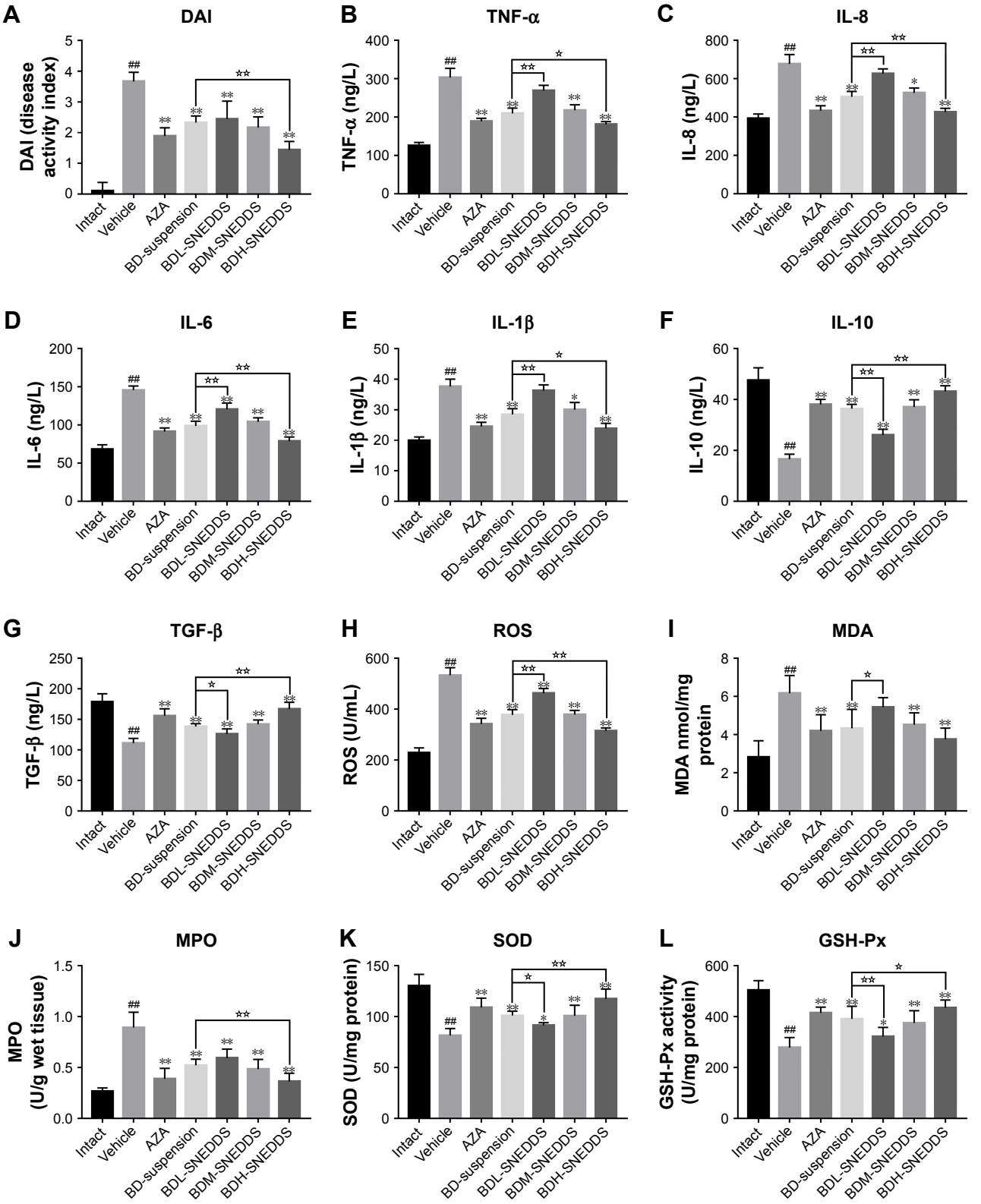

Figure 6 (**A**) Disease activity index. (**B–L**) Effects of BD-SNEDDS on colon levels of inflammatory cytokines and oxidative stress.

Notes: Data are expressed as mean±SD and analyzed by ANOVA followed by Dunnett's test. $^{\#\#}P<0.01$ vs intact group, $^{**}P<0.01$ and $^{*}P<0.05$ vs the vehicle group, $^{\star}P<0.05$ and $^{\star\star}P<0.01$ vs BD-suspension group.

Abbreviations: BD-SNEDDS, BD-loaded self-nanoemulsifying drug delivery system; BD-suspension, BD suspended in 0.5% sodium carboxymethyl cellulose solution; DAI, disease activity index; TNF-α, tumor necrosis factor-α; IL-1β, IL-6, IL-8, and IL-10, interleukin-1β, -6, -8 and -10; TGF-β, transforming growth factor-β; SOD, superoxide dismutase; MDA, malondialdehyde; MPO, myeloperoxidase; GSH-Px, glutathione peroxidase; ROS, reactive oxygen species; AZA, azathioprine; BDL-SNEDDS, low-dosage BD-loaded self-nanoemulsifying drug delivery system; BDM-SNEDDS, medium-dosage BD-loaded self-nanoemulsifying drug delivery system; BDH-SNEDDS, high-dosage BD-loaded self-nanoemulsifying drug delivery system.

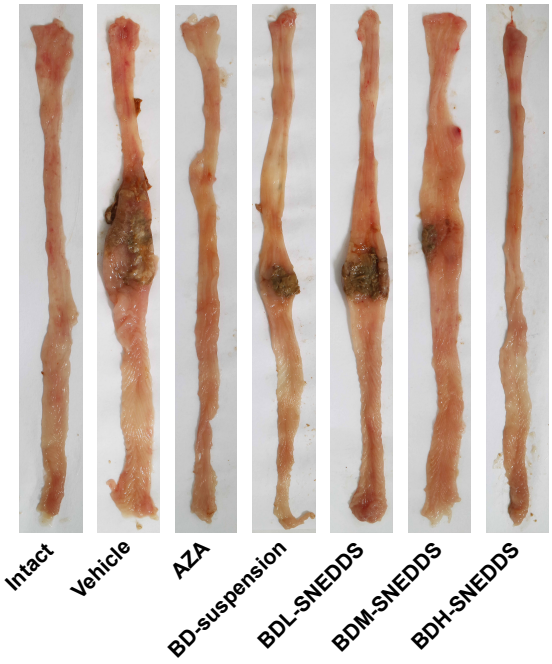

Figure 7 Effects of BD-SNEDDS on macroscopic changes in TNBS-induced UC in rats.
Note: Data are expressed as mean±SD (n=6).
Abbreviations: BD-SNEDDS, BD-loaded self-nanoemulsifying drug delivery system; AZA, azathioprine; TNBS, trinitrobenzenesulfonic acid; UC, ulcerative colitis; BDL-SNEDDS, low-dosage BD-loaded self-nanoemulsifying drug delivery system; BDM-SNEDDS, medium-dosage BD-loaded self-nanoemulsifying drug delivery system; BDH-SNEDDS, high-dosage BD-loaded self-nanoemulsifying drug delivery system.

disappearance of crypt structure, and enterocyte loss, resulting in a low microscopic score (Figure 5A). On the contrary, BD-SNEDDS, BD-suspension, and positive drug effectively restored crypt architecture epithelium and reduced histologic inflammation. The beneficial effect in attenuating deteriorating pathologies was also observed in the BDH-SNEDDS group (3 mg/kg) ($P<0.01$). BD-suspension (3 mg/kg) group exerted a similar therapeutic effect to BDM-SNEDDS group ($P>0.05$). These results indicated that BD exhibited strong potency against TNBS-induced colitis in a dose- and formulation-dependent manner.

Effects of BD-SNEDDS on inflammatory cytokines

Pro-inflammatory cytokines (IL-1β, IL-6, IL-8, and TNF-α) levels were significantly increased in TNBS-treated rats compared with the intact group (Figure 6B–E; $P<0.01$). Administration of BD or the positive drug dramatically suppressed the levels of these pro-inflammatory cytokines. On the contrary, the anti-inflammatory cytokines including IL-10 and TGF-β were decreased to a low level after TNBS exposure, whereas treatment with middle- or high-dose of BD-SNEDDS, BD-suspension, or AZA notably restored these anti-inflammatory cytokines (Figure 6F–G; $P<0.01$). Compared with BD-suspension, BDH-SNEDDS displayed substantially greater effects in suppressing pro-inflammatory cytokines and promoting anti-inflammatory cytokines ($P<0.05$). In the attenuation of inflammatory cytokines, BD-suspension showed similar effects to BDM-SNEDDS.

Effects of BD-SNEDDS on oxidative stress

Oxidative stress is highly correlated with the process of colon inflammation. As shown in Figure 6H–L, MPO, MDA, and ROS levels were significantly increased in the TNBS group, while SOD and GSH-Px activities were markedly decreased in comparison to the intact group ($P<0.01$). However, the MPO, MDA, and ROS levels were significantly suppressed by AZA and BD treatments ($P<0.05$). These test particles (AZA and BD) could relieve the oxidative stress by increasing SOD and GSH-Px contents, and there was significant statistical difference ($P<0.05$) between the BDH-SNEDDS and BD-suspension in reducing oxidative stress.

Effects of BD-SNEDDS on NF-κB p65 protein expression in colon tissues

TNBS administration substantially increased the expression of NF-κB p65 ($P<0.01$; Figure 8), while BD-SNEDDS markedly reversed this trend ($P<0.01$ vs TNBS group) in a dose-dependent manner. At the same dose of BD, BDH-SNEDDS displayed superior effect in suppressing NF-κB p65 expression than BD-suspension.

Effects of BD-SNEDDS on *iNOS* and *COX-2* mRNA expressions

The mRNA expressions of *iNOS* and *COX-2* significantly increased after dextran sulfate sodium induction compared with the normal group (Figure 9). However, these alternations were significantly prohibited by BD-SNEDDS in a dose-dependent manner ($P<0.01$).

Effects of BD-SNEDDS on the colonic levels of TLR4, MyD88, TRAF6, and NF-κB p65

NF-κB, an important pro-inflammatory factor, plays a key role in UC.[33] To investigate the potential anti-UC mechanism of BD-SNEDDS in TNBS-induced colitis rats, we examined the effects of BD-SNEDDS on the expressions of TLR4, MyD88, TRAF6, and NF-κB by Western blot analysis. As illustrated in Figure 10, TLR4, MyD88, TRAF6, and NF-κB total proteins were upregulated in the colon tissue compared with the intact control ($P<0.01$), whereas treatment with different doses of BD-SNEDDS significantly suppressed the

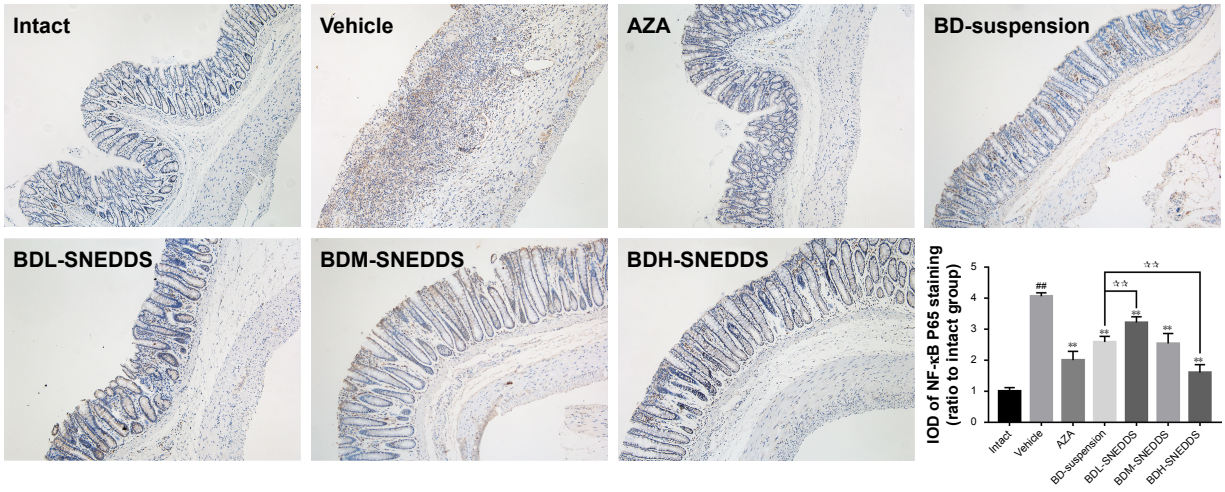

Figure 8 Effects of BD-SNEDDS on the protein expression of NF-κB in rats with TNBS-induced UC (immunohistochemistry analysis of colorectal sections; original magnification 100×).

Notes: The IOD is expressed as mean±SD and analyzed by ANOVA followed by Dunnett's test. ##$P<0.01$ vs intact group, **$P<0.01$ vs vehicle group, ☆☆$P<0.01$ vs BD-suspension group.

Abbreviations: BD-SNEDDS, BD-loaded self-nanoemulsifying drug delivery system; BD-suspension, BD suspended in 0.5% sodium carboxymethyl cellulose solution; IOD, integrated optical density; AZA, azathioprine; TNBS, trinitrobenzenesulfonic acid; NF-κB, nuclear factor-κB; UC, ulcerative colitis; BDL-SNEDDS, low-dosage BD-loaded self-nanoemulsifying drug delivery system; BDM-SNEDDS, medium-dosage BD-loaded self-nanoemulsifying drug delivery system; BDH-SNEDDS, high-dosage BD-loaded self-nanoemulsifying drug delivery system.

expression of TLR4 in a dose-dependent manner ($P<0.05$). MyD88, TRAF6, and NF-κB expression levels were significantly reduced by medium and high doses of BD-SNEDDS and AZA ($P<0.05$).

Discussion

The desiccative ripe fruit of *B. javanica* is traditionally utilized as a therapy for dysentery in TCM.[34] Nowadays, most research on *B. javanica* focuses on anti-cancer properties; however, less attention has been paid to its traditional applications such as dysentery.

BD is a quassinoid isolated from the seeds of *B. javanica*. This natural compound has been found to exhibit various promising pharmacological properties. Our pilot studies showed that BD could effectively alleviate TNBS-induced UC in rats. However, oral administration of BD faces a plight of low aqueous solubility and low bioavailability, which largely limits its medicinal application in clinical practice.

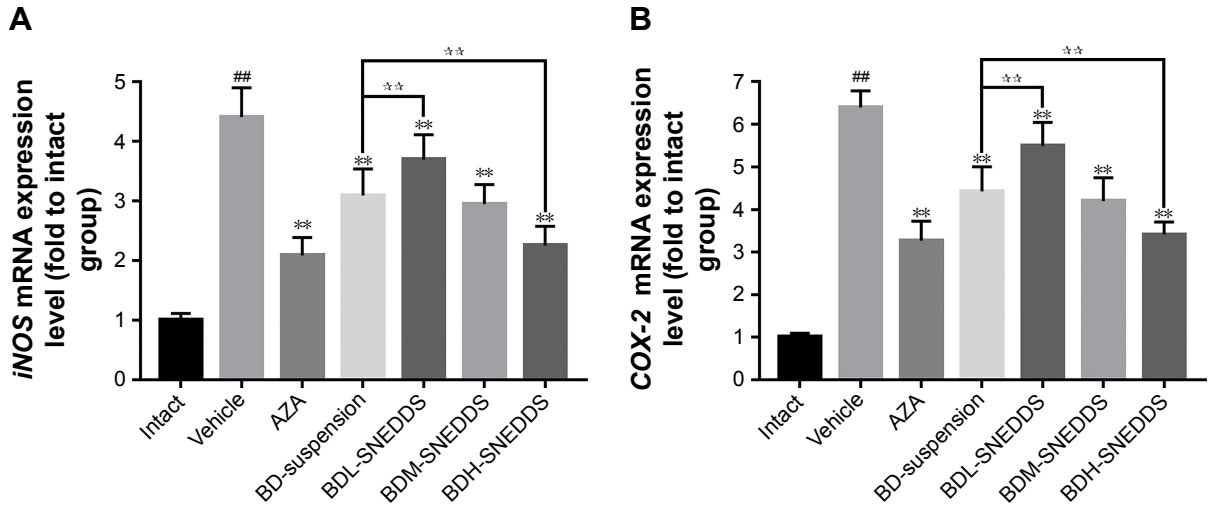

Figure 9 The mRNA expression levels of *iNOS* (**A**) and *COX-2* (**B**) in rats with TNBS-induced UC.

Notes: Results are expressed as the means±SD and analyzed by ANOVA followed by Dunnett's test (n=6). ##$P<0.01$ vs vehicle group; **$P<0.01$ vs vehicle group; ☆☆$P<0.01$ vs BD-suspension group.

Abbreviations: BD-SNEDDS, BD-loaded self-nanoemulsifying drug delivery system; BD-suspension, BD suspended in 0.5% sodium carboxymethyl cellulose solution; *iNOS*, inducible nitric oxide synthase; *COX-2*, cyclooxygenase-2; *GAPDH*, glyceraldehyde-3-phosphate dehydrogenase; AZA, azathioprine; TNBS, trinitrobenzenesulfonic acid; UC, ulcerative colitis; BDL-SNEDDS, low-dosage BD-loaded self-nanoemulsifying drug delivery system; BDM-SNEDDS, medium-dosage BD-loaded self-nanoemulsifying drug delivery system; BDH-SNEDDS, high-dosage BD-loaded self-nanoemulsifying drug delivery system.

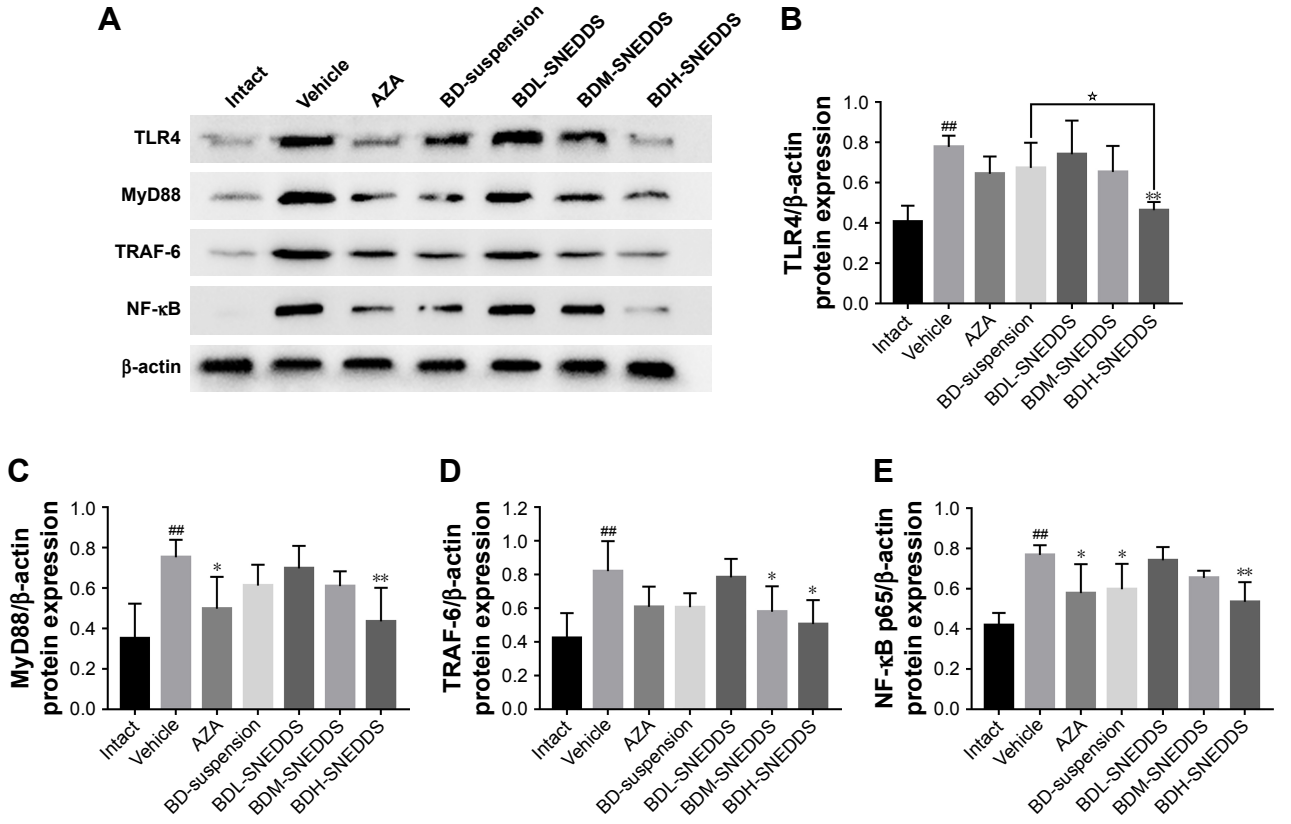

Figure 10 Effects of BD-SNEDDS on the protein expressions of TLR4, MyD88, TRAF-6, and NF-κB p65 in colonic tissue by Western blot.

Notes: (**A**) Representative Western blot images of TLR4, MyD88, TRAF-6, and NF-κB p65 protein expressions in TNBS-induced colonic tissues. Protein expression levels of TLR4 (**B**), MyD88 (**C**), TRAF-6 (**D**), and NF-κB p65 (**E**) in colonic tissue. Data are presented as mean±SD (n=3). $^{\#\#}P<0.01$ vs intact group, $^{*}P<0.05$ and $^{**}P<0.01$ vs vehicle group, $^{*}P<0.05$ vs BD-suspension group.

Abbreviations: BD-SNEDDS, BD-loaded self-nanoemulsifying drug delivery system; BD-suspension, BD suspended in 0.5% sodium carboxymethyl cellulose solution; TLR4, toll-like receptor 4; MyD88, myeloid differentiation primary response 88; TRAF-6, TNF receptor-associated factor 6; NF-κB, nuclear factor-kappa B; AZA, azathioprine; TNBS, trinitrobenzenesulfonic acid; BDL-SNEDDS, low-dosage BD-loaded self-nanoemulsifying drug delivery system; BDM-SNEDDS, medium-dosage BD-loaded self-nanoemulsifying drug delivery system; BDH-SNEDDS, high-dosage BD-loaded self-nanoemulsifying drug delivery system.

Therefore, it is necessary to break these predicaments by exploring a suitable drug delivery system to improve its aqueous solubility and bioavailability, as well as to minimize adverse reactions.

In recent years, nano-sized drug delivery system have become a promising strategy which has been widely used in treatment of UC.[35–37] SNEDDS, a promising drug delivery system, contains various advantages including improved long-term storage stability, increased drug efficacy, reduced side effects, and enhanced bioavailability.[17] Because of convenient manufacturing, improved drug bioavailability, and lack of toxicity, SNEDDS has been recognized as a promising drug carrier.

In order to search for an appropriate formulation for BD with outstanding emulsifying ability and low side effects, we screened various surfactants, cosurfactants, and oils. In terms of surfactants, an optimized surfactant to emulsify the oil spontaneously to form SNEDDS is preferred to be nonionic (being less toxic), water-soluble, and has a HLB of 12–18.[5] HS-15 is a nonionic surfactant consisting of monoesters and diesters of 12-hydroxystearic acid, with HLB value between 12 and 14. HS-15 is a safe surfactant with short formation time of self-emulsification.[38] Additionally, HS-15 with a suitable HLB value is favorable to form the smallest globule size nanoemulsion.[39]

Other nonionic surfactants, such as Tweens and Cremophor RH40 and Pluronic F68, are widely employed to improve the dissolution and delivery of drugs.[40,41] Tween 80, a polyoxyethylene sorbitan monooleate (average HLB value of 15), has been deemed as a low-cost and powerful emulsifier.[42–44] Cremophor RH40, a polyoxyl 40 hydrogenated castor oil (HLB value ranging 14–16), is an efficient emulsifier used to formulate several drugs such as paclitaxel and teniposide.[44] Pluronic F68 (Poloxamer 188), a PEO–PPO–PEO-triblock copolymer (HLB value of 29), is known to enhance the drug solubility and formulation stability in drug delivery system.[45,46] Among the various selected surfactants, HS-15 was therefore selected as the surfactant in

formulating SNEDDS, as it exhibited high solubility of BD and the smallest droplet size.

From the results obtained, even though the HLB values were similar, a wide difference was observed in the emulsion droplet size between different emulsifiers. The observation indicated that droplet size of the emulsions generated from SNEDDS seemed to be independent of the HLB of the emulsifier. By contrast, the structure of the emulsifier was found to significantly influence the emulsion droplet size. Hence, it could be deduced that the droplet size might depend primarily on the emulsifier molecular structure.

The concentration of surfactants is one of the key elements in forming emulsion.[18] A higher proportion of surfactant has been proposed to cause smaller mean droplet or particle size that favors faster emulsification.[47] However, higher concentrations of surfactants might cause irritation to the GI mucosa. Surfactant concentration in SNEDDS should be kept at a minimal level as far as possible.[17] In the present study, the S_{mix} ratio of 2:1 resulted in small droplet size and PDI, and no significant change of droplet size was observed when the ratio of S_{mix} was greater than 2:1. Therefore, the S_{mix} ratio of 2:1 was selected to form SNEDDS.

An appropriate cosurfactant provides sufficient flexibility to the interfacial film to take up different curvatures which is important for SNEDDS formulations.[38] Cosurfactant is commonly employed in SNEDDS formulation to reduce interfacial tension.[39,48,49] Propylene glycol is a kind of frequently used cosurfactant in nano-formulation, indicating efficient spontaneous nanoemulsion.[50–52] In the present work, propylene glycol exerted the strongest dissolving capacity for BD among all other cosurfactants.

In the oils test, BD was found to have maximum solubility in MCT. Our result also indicated that MCT resulted in the smallest droplet size and PDI compared with other selected oils. MCT is commonly served as a dispersible and absorbable lipid-solubilizing agent. This property enhances lymphatic transport of drug and avoids degradation by first-pass hepatic metabolism to improve bioavailability.[53] To obtain an optimum drug loading, form the smallest particles, and improve lymphatic transport of BD, MCT was selected as the oil phase in preparing BD-SNEDDS. Thus, HS-15, MCT, propylene glycol, and water were selected as the surfactant, oil phase, cosurfactant, and pseudo-ternary phase, respectively. Based on the results of pseudo-ternary phase diagram, HS-15, propylene glycol, and MCT at a weight ratio of 4:2:1 (w/w/w) were used for the integration of SNEDDS.

Droplet size is an important parameter indicating formulation performance. As shown in droplet size determination and TEM images, BD-SNEDDS exhibited a homogeneous morphology. ZP is an electrokinetic potential at the slipping/shear plane of a colloid droplet moving under electric field in colloidal systems and nano-medicines.[54] As an important indicator of stability, ZP is widely used to evaluate the stability of nanoemulsion system.[55–57] Higher ZP of nanoemulsion indicates a higher stabilization to avoid degradation and aggregation.[58] In a general way, ZP values of nanoemulsions above ±30 mV represent a relatively good stability.[59] PDI is an assessment index of the dispersion of droplet size distribution. As a general rule, PDI value ranges from 0 to 1. PDI values <0.3 indicate narrow distribution. Our results demonstrated that BD-SNEDDS could self-emulsify to form nano-emulsion when gently agitated with distilled water. Furthermore, the BD-SNEDDS formulation exhibited a higher negative average ZP, which showed a favorable stability. Consistently, the PDI value of 0.045±0.0098 indicated the homogeneity of droplet size.[60–62]

Next, we evaluated the stability of BD-SNEDDS in simulated harsh GI environment. In general, nano-sized spheres of SNEDDS indicate a huge surface area and surface energy, which may lead to physical and chemical instability under different conditions of pH, temperature change, or gravitational force. Therefore, evaluation of dilution stability and thermodynamic stability of BD-SNEDDS is of vital importance. The stability results demonstrated that BD-SNEDDS had satisfactory physicochemical stability, which indicated it could remain stable in different storage environments and harsh GI environment.

The in vitro release profile of BD-SNEDDS formulation was evaluated by using dialysis bag to determine the release behavior. The release of BD from BD-SNEDDS in simulated intestinal fluid (pH 6.8) was significantly higher than that from BD suspension. Possible reasons include the following: 1) small droplet size of SNEDDS provided a large surface area for drug release into the aqueous phase; 2) BD might readily pass through dialysis membrane with the oil phase in SNEDDS;[63] 3) release of BD from SNEDDS into the simulated gastric fluid (pH 1.2) was slower than that from suspension. This nature might allow BD-SNEDDS to survive in the harsh gastric environment and release in the intestine. These results indicated the crucial role of SNEDDS in enhancing BD solubilization and in vitro release, which may affect the bioavailability of BD.

Based on the results mentioned above, we further evaluated the in vivo bioavailability of BD-SNEDDS. From the results, the higher values of C_{max} observed in BD-SNEDDS were consistent with the prior in vitro finding. In addition,

compared with the free drug suspension, higher AUC_{0-24} was observed in BD-SNEDDS formulation, indicating improved absorption of BD from the GI tract.[64] Compared with the BD-suspension, $t_{1/2}$ was significantly prolonged, suggesting that BD in SNEDDS could stay longer in the body. The better pharmacokinetic parameters observed with BD-SNEDDS in comparison to BD-suspension might be due to the small droplet size that forms a large interfacial surface area for drug penetration into epithelial cells and enhanced absorption.[55] Furthermore, it has been reported that a larger portion of formulas with long- and medium-chain fatty acids have the ability to by-pass portal circulation via lymphatic transport.[65] The presence of MCT enhances lipoprotein synthesis and subsequent lymphatic absorption.[66] Nevertheless, the exact mechanism merited further investigation.

In the present study, we evaluated the anti-colitis efficacy of BD-SNEDDS in parallel to BD-suspension. Using the TNBS-induced model,[67,68] we assessed the clinical symptoms including body weight loss, diarrhea, hematochezia, DAI, histological alterations, and shortened colons. The DAI score is a common indicator for the evaluation of severity of colitis, wherein a higher DAI score represents more discomfort conditions.[69] It was found that TNBS-induced colitis rats exhibited dramatic body weight loss, higher DAI score, and shorter colon length compared with the control group. However, rats treated with BD-SNEDDS exhibited a notable therapeutic effect, resulting in attenuated loss of body weight, decreased intestinal bleeding, and reduced DAI score in a dose-dependent manner. Furthermore, the salutary effect of BD-SNEDDS was further confirmed by histological observation. Mucosal damage and infiltration of inflammatory cells were significantly ameliorated by BD-SNEDDS treatment. It is noteworthy that BD-SNEDDS had advanced therapeutic effect compared with the positive drug and BD-suspension. All these results suggested that the improved pharmacokinetic properties by SNEDDS might significantly contribute to the beneficial therapeutic effects of BD against UC.

UC is a chronic and relapsing inflammatory disease. Under UC attack, imbalanced release of cytokines results in inflammation and damage of intestinal mucosa. It has been generally accepted that various cytokines are considered crucial signals in the intestinal immune system.[70] As key pro-inflammatory mediators, TNF-α, IL-8, IL-1β, and IL-6 cause intestinal mucosal impairment resulting in inflammation.[70,71] Elevated levels of the pro-inflammatory cytokines, such as IL-1β and TNF-α, are present in the gut mucosa of patients suffering from UC. The cytokines TNF-α and IL-1β have been intimately related to the stimulation of the production of IL-8 during the pathogenesis of UC.[72] Blocking the productions of these cytokines can effectively ameliorate inflammation in colitis rats. The cytokines IL-10 and TGF-β, known as strong immunosuppressive and immunoregulatory factors, could effectively inhibit pro-inflammatory cytokine synthesis and antigen presentation, leading to alleviation of inflammation responses.[73] In our experiments, BD-SNEDDS dramatically inhibited TNBS-induced production of TNF-α, IL-8, IL-1β, and IL-6 and substantially promoted the production of immune-regulatory mediators in a dose-dependent manner. High dose of BD-SNEDDS had a better anti-inflammatory effect than middle- and low-dose counterparts, positive drugs, and BD-suspension. These results indicated that the ameliorative effects of BD-SNEDDS against TNBS-induced colitis might be closely related to the decrease of infiltration of inflammatory cells and attenuation of the mucosal damage.

The increase of inflammatory cells and disruption of the mucosal immune response cause accumulation of oxidative stress which inflicts intestinal injuries in UC.[74] Oxidative stress and its consequent lipid peroxidation are known to damage cellular macromolecules such as DNA, lipids, and proteins, which could exacerbate free radical chain reactions and activate the release of pro-inflammatory mediators, disrupt the integrity of the intestinal mucosal barrier, and activate inflammatory mediators.[75] MPO is an enzyme abundantly found in neutrophils which has been used as a marker of cell-specific infiltration and the severity of inflammation.[76] As a marker for free radicals-induced lipid peroxidation, MDA is widely used as a biochemical marker of oxidative stress.[77] ROS is the natural product of aerobic metabolism of animal and human cells, which is implicated as a mediator of intestinal inflammation and plays a vital role in the pathophysiology of UC.[78] Overproduction of ROS in intestinal mucosal cells induces the immune response, which leads to the injury of intestinal epithelial cells, disruption of integrity of the intestinal barrier, and initiation of the intestinal inflammation.[79] It is involved in anti-inflammation process and cleared by a series of constitutively expressed antioxidant enzymes, such as SOD and GSH-Px. These two enzymes can counteract the overaccumulation of ROS.[80] Therefore, measurement of enzymatic activities can manifest acute intestinal inflammation.

Hence, we evaluated the potential effect of BD-SNEDDS on antioxidant enzymes including SOD and GSH-Px, as well as ROS, MPO, and MDA levels. In this study, the decrease of SOD and GSH-Px after TNBS treatment was found to be noticeably inhibited by BD-SNEDDS treatment, while the levels of ROS, MPO, and MDA were

suppressed significantly. All the results indicated that the amelioration of histopathological deterioration might be intimately associated with the positive regulation of anti-oxidative and anti-inflammatory status by BD-SNEDDS treatment.

Meanwhile, our real-time PCR results indicated that BD-SNEDDS exerted better anti-inflammatory effects by regulating the expression of several important enzymes. BD-SNEDDS effectively suppressed COX-2, which was upregulated in colitis,[81] and iNOS, which produced nitric oxide (NO) during the pathogenesis of colitis.[82] It is hypothesized that downregulation of *iNOS* and *COX-2* gene expression by BD-SNEDDS might be tightly related to the suppression of NF-κB activation.[83]

TLR4/NF-κB pathway has been found to be closely related to the immune system and anti-inflammatory signaling pathways, in recent years.[71] The MyD88-dependent TLR4 signaling pathway is one of major signaling pathways in stimulating the production of NF-κB by activating TRAF6.[33] As a member of the toll-like receptors (TLRs) family, TLR4 can mediate the transport of signal factors across the plasma membrane.[84] TLR4 triggers the recruitment of the downstream regulator MyD88 which induces NF-κB expression and ultimately results in inflammatory response.[85] In the present study, we demonstrated that the upregulated protein expressions of TLR4, MyD88, TRAF6, and NF-κB after TNBS induction were largely attenuated by BD-SNEDDS or BD-suspension treatment. These results suggested that TLR4/NF-κB signaling pathway was at least partially involved in the BD-initiated anti-colitis effects.

In conclusion, our results provide experimental evidence for the traditional application of *B. javanica* in the treatment of dysentery. This is the first report on the regulation of TLR4-linked NF-κB signaling pathway by C20 quassinoids, and also the pioneer study illuminating the anti-UC activity and action mechanism of C20 quassinoids. For the first time, BD is found to exert similar anti-UC activity as the current first-line antidote AZA, with much lower dosage. The profound therapeutic efficacy of BD against UC is further improved by SNEDDS-mediated physicochemical optimization. We consider this study as a good example in developing effective UC treatments with SNEDDS from traditional herbal remedies. Our optimized formulation of SNEDDS may represent a promising drug carrier for improving the physiochemical properties and enhancing the bioactivities of BD and many other analogous quassinoids. However, more detailed mechanisms for anti-inflammatory effects of BD on colitis are heavily merited. The current results provided a foundation and justification for further research of this new drug delivery system for conventional medications.

Conclusion

The SNEDDS helps overcome the inadequate bioavailability challenges of BD by favorably improving physicochemical properties, enhancing drug assimilation, and prolonging the in vivo retention time. The present study demonstrates that BD in SNEDDS possesses strong anti-inflammatory effects against colonic inflammation in rats via inhibition of inflammatory mediators and oxidative stress and downregulation of TLR4-linked NF-κB transduction pathways. Compared with BD suspension, BD-SNEDDS significantly improves oral bioavailability and enhances anti-colitis efficiency. Thus, this system represents promising potential for new drug development for UC treatment.

Acknowledgments

This work was supported by Science and Technology Planning Project of Guangdong Province, China (grant no 2017A050506044), Science and Technology Planning Project of Guangzhou, Guangdong, China (grant no 201704030028), and Natural Science Foundation of Guangdong Province, China (grant no 2018A030313408).

Disclosure

The authors report no conflicts of interest in this work.

References

1. Turner D, Levine A, Escher JC, et al. Management of pediatric ulcerative colitis: joint ECCO and ESPGHAN evidence-based consensus guidelines. *J Pediatr Gastroenterol Nutr*. 2012;55(3):340–361.
2. Romero M, Vera B, Galisteo M, et al. Protective vascular effects of quercitrin in acute TNBS-colitis in rats: the role of nitric oxide. *Food Funct*. 2017;8(8):2702–2711.
3. Gu P, Zhu L, Liu Y, Zhang L, Liu J, Shen H, Protective SH. Protective effects of paeoniflorin on TNBS-induced ulcerative colitis through inhibiting NF-kappaB pathway and apoptosis in mice. *Int Immunopharmacol*. 2017;50:152–160.
4. Bitton A, Vutcovici M, Patenaude V, Sewitch M, Suissa S, Brassard P. Epidemiology of inflammatory bowel disease in Québec: recent trends. *Inflamm Bowel Dis*. 2014;20(10):1770–1776.
5. Ukil A, Maity S, Das PK. Protection from experimental colitis by theaflavin-3,3′-digallate correlates with inhibition of IKK and NF-kappaB activation. *Br J Pharmacol*. 2006;149(1):121–131.
6. Wang P, Zhao S, Feng J, Zhao H, Wang Q, Kuang H. Advances in studies on Chinese materia medica for treatment of ulcerative colitis based on NF-kappaB signal pathway. *Chinese Traditional and Herbal Drugs*. 2015;46(10):1556–1561.
7. Kamperdick C, Sung TV, Thuy TT, Van Tri M, Adam G, Thuy TT. (20R)-O-(3)-α-l-arabinopyranosyl-pregn-5-en-3β,20-diol from Brucea javanica. *Phytochemistry*. 1995;38(3):699–701.
8. Huang YF, Zhou JT, Qu C, et al. Anti-inflammatory effects of Brucea javanica oil emulsion by suppressing NF-κB activation on dextran sulfate sodium-induced ulcerative colitis in mice. *J Ethnopharmacol*. 2017;198:389–398.

9. Liu L, Lin ZX, Leung PS, Chen LH, Zhao M, Liang J. Involvement of the mitochondrial pathway in bruceine D-induced apoptosis in Capan-2 human pancreatic adenocarcinoma cells. *Int J Mol Med*. 2012; 30(1):93.
10. Lau ST, Lin ZX, Liao Y, Zhao M, Cheng CH, Leung PS. Bruceine D induces apoptosis in pancreatic adenocarcinoma cell line PANC-1 through the activation of p38-mitogen activated protein kinase. *Cancer Lett*. 2009;281(1):42–52.
11. Xiao Z, Ching Chow S, Han Li C, et al. Role of microRNA-95 in the anticancer activity of Brucein D in hepatocellular carcinoma. *Eur J Pharmacol*. 2014;728:141–150.
12. Pan L, Zheng F, Zhu H, Zhang S, Yan HU. The effect of Bruceine D on high-risk human papillomavirus 16 infected cell and its possible mechanism. *Journal of Wenzhou Medical University*. 2015.
13. Hall IH, Lee KH, Imakura Y, Okano M, Johnson A. Anti-inflammatory agents III: Structure-activity relationships of brusatol and related quassinoids. *J Pharm Sci*. 1983;72(11):1282–1284.
14. Kesarwani K, Gupta R, Mukerjee A. Bioavailability enhancers of herbal origin: an overview. *Asian Pac J Trop Biomed*. 2013;3(4):253–266.
15. dal Mas J, Zermiani T, Thiesen LC, et al. Nanoemulsion as a carrier to improve the topical anti-inflammatory activity of stem bark extract of *Rapanea ferruginea*. *Int J Nanomedicine*. 2016;11:4495–4507.
16. Huang Y, Zhao Y, Liu F, Liu S. Nano Traditional Chinese Medicine: Current Progresses and Future Challenges. *Curr Drug Targets*. 2015;16(13):1548–1562.
17. Date AA, Desai N, Dixit R, Nagarsenker M. Self-nanoemulsifying drug delivery systems: formulation insights, applications and advances. *Nanomedicine*. 2010;5(10):1595–1616.
18. Wang L, Dong J, Chen J, Eastoe J, Li X. Design and optimization of a new self-nanoemulsifying drug delivery system. *J Colloid Interface Sci*. 2009;330(2):443–448.
19. Li X, Wang L, Wang B. Optimization of encapsulation efficiency and average particle size of Hohenbuehelia serotina polysaccharides nanoemulsions using response surface methodology. *Food Chem*. 2017; 229:479–486.
20. Man F, Choo CY. HPLC-MS/MS method for bioavailability study of bruceines D & E in rat plasma. *J Chromatogr B Analyt Technol Biomed Life Sci*. 2017;1063:183–188.
21. Lai ZQ, Ip SP, Liao HJ, et al. Brucein D, a Naturally Occurring Tetracyclic Triterpene Quassinoid, Induces Apoptosis in Pancreatic Cancer through ROS-Associated PI3K/Akt Signaling Pathway. *Front Pharmacol*. 2017;8:936.
22. Ashizuka S, Inatsu H, Kita T, Kitamura K. Adrenomedullin Therapy in Patients with Refractory Ulcerative Colitis: A Case Series. *Dig Dis Sci*. 2016;61(3):872–880.
23. Sun P, Zhou K, Wang S, et al. Involvement of MAPK/NF-kappa B Signaling in the Activation of the Cholinergic Anti-Inflammatory Pathway in Experimental Colitis by Chronic Vagus Nerve Stimulation. *PLos One*. 2013;8(8):e69424.
24. Bell CJ, Gall DG, Wallace JL. Disruption of colonic electrolyte transport in experimental colitis. *Am J Physiol*. 1995;268(4 Pt 1):G622–G630.
25. Ameho CK, Adjei AA, Harrison EK, et al. Prophylactic effect of dietary glutamine supplementation on interleukin 8 and tumour necrosis factor alpha production in trinitrobenzene sulphonic acid induced colitis. *Gut*. 1997;41(4):487–493.
26. Li X, Wu L, Konda Y, et al. Bruceines D, E and H. *Journal of Heterocyclic Chemistry*. 1989;26(2):493–501.
27. Hou J, Sun E, Sun C, et al. Improved oral bioavailability and anticancer efficacy on breast cancer of paclitaxel via Novel Soluplus(®)-Solutol(®) HS15 binary mixed micelles system. *Int J Pharm*. 2016; 512(1):186–193.
28. Hou J, Wang J, Sun E, et al. Preparation and evaluation of icariside II-loaded binary mixed micelles using Solutol HS15 and Pluronic F127 as carriers. *Drug Deliv*. 2016;23(9):3248–3256.
29. Kim KT, Lee JY, Park JH, Cho HJ, Yoon IS, Kim DD. Capmul MCM/Solutol HS15-Based Microemulsion for Enhanced Oral Bioavailability of Rebamipide. *J Nanosci Nanotechnol*. 2017;17(4):2340–2344.
30. Panatieri LF, Brazil NT, Faber K, et al. Nanoemulsions Containing a Coumarin-Rich Extract from Pterocaulon balansae (Asteraceae) for the Treatment of Ocular Acanthamoeba Keratitis. *AAPS PharmSciTech*. 2017;18(3):721–728.
31. Surh J, Decker EA, Mcclements DJ. Utilisation of spontaneous emulsification to fabricate lutein-loaded nanoemulsion-based delivery systems: factors influencing particle size and colour. *Int J Food Sci Technol*. 2017;52(6):1408–1416.
32. Zhong J, Liu X, Wang Y, Qin X, Li Z. γ-Oryzanol nanoemulsions produced by a low-energy emulsification method: an evaluation of process parameters and physicochemical stability. *Food Funct*. 2017;8(6): 2202–2211.
33. Fei L, Xu K. Zhikang Capsule ameliorates dextran sodium sulfate-induced colitis by inhibition of inflammation, apoptosis, oxidative stress and MyD88-dependent TLR4 signaling pathway. *J Ethnopharmacol*. 2016;192:236–247.
34. Shanzi H. *The Progress of Traditional Chinese Medicine Treatment in Ulcerative Colitis*. Beijing: University of Chinese Medicine; 2014.
35. Collnot EM, Ali H, Lehr CM. Nano- and microparticulate drug carriers for targeting of the inflamed intestinal mucosa. *J Control Release*. 2012;161(2):235–246.
36. Schmidt C, Lautenschlaeger C, Collnot EM, et al. Nano- and microscaled particles for drug targeting to inflamed intestinal mucosa: a first in vivo study in human patients. *J Control Release*. 2013;165(2):139–145.
37. Laroui H, Wilson DS, Dalmasso G, et al. Nanomedicine in GI. *Am J Physiol Gastrointest Liver Physiol*. 2011;300(3):G371–G383.
38. Sharma S, Narang JK, Ali J, Baboota S. Synergistic antioxidant action of vitamin E and rutin SNEDDS in ameliorating oxidative stress in a Parkinson's disease model. *Nanotechnology*. 2016;27(37):375101.
39. Dash RN, Mohammed H, Humaira T, Ramesh D, Habibuddin M. Design, optimization and evaluation of glipizide solid self-nanoemulsifying drug delivery for enhanced solubility and dissolution. *Saudi Pharm J*. 2015;23(5):528–540.
40. Strickley RG. Solubilizing excipients in oral and injectable formulations. *Pharm Res*. 2004;21(2):201–230.
41. Juretić M, Cetina-Čižmek B, Filipović-Grčić J, Hafner A, Lovrić J, Pepić I. Biopharmaceutical evaluation of surface active ophthalmic excipients using in vitro and ex vivo corneal models. *Eur J Pharm Sci*. 2018;120:133–141.
42. Jin W, Chen L, Hu M, et al. Tween-80 is effective for enhancing steam-exploded biomass enzymatic saccharification and ethanol production by specifically lessening cellulase absorption with lignin in common reed. *Applied Energy*. 2016;175:82–90.
43. Cheng M, Zeng G, Huang D, et al. Tween 80 surfactant-enhanced bioremediation: toward a solution to the soil contamination by hydrophobic organic compounds. *Crit Rev Biotechnol*. 2018;38(1):17–30.
44. Kiss L, Walter FR, Bocsik A, et al. Kinetic analysis of the toxicity of pharmaceutical excipients Cremophor EL and RH40 on endothelial and epithelial cells. *J Pharm Sci*. 2013;102(4):1173–1181.
45. Mahaling B, Srinivasarao DA, Raghu G, Kasam RK, Bhanuprakash Reddy G, Katti DS. A non-invasive nanoparticle mediated delivery of triamcinolone acetonide ameliorates diabetic retinopathy in rats. *Nanoscale*. Epub 2018 Jun 13.
46. Yordanov G, Skrobanska R, Petkova M. Poly(butyl cyanoacrylate) nanoparticles stabilised with poloxamer 188: particle size control and cytotoxic effects in cervical carcinoma (HeLa) cells. *Chemical Papers*. 2016;70(3):365–374.
47. Boakye CH, Patel K, Patel AR, et al. Lipid-based oral delivery systems for skin deposition of a potential chemopreventive DIM derivative: characterization and evaluation. *Drug Deliv Transl Res*. 2016;6(5): 526–539.
48. Shen J, Bi J, Tian H, et al. Preparation and evaluation of a self-nanoemulsifying drug delivery system loaded with Akebia saponin D-phospholipid complex. *Int J Nanomedicine*. 2016;11:4919–4929.
49. Zhao Y, Wang C, Chow AH, et al. Self-nanoemulsifying drug delivery system (SNEDDS) for oral delivery of Zedoary essential oil: formulation and bioavailability studies. *Int J Pharm*. 2010;383(1–2):170–177.

50. Patel G, Shelat P, Lalwani A, Modeling S. Statistical modeling, optimization and characterization of solid self-nanoemulsifying drug delivery system of lopinavir using design of experiment. *Drug Deliv*. 2016; 23(8):3027–3042.
51. Puri R, Mahajan M, Sahajpal NS, Singh H, Singh H, Jain SK. Self-nanoemulsifying drug delivery system of docosahexanoic acid: development, in vitro, in vivo characterization. *Drug Dev Ind Pharm*. 2016; 42(7):1032–1041.
52. Salem HF, Kharshoum RM, Halawa AKA, Naguib DM. Preparation and optimization of tablets containing a self-nano-emulsifying drug delivery system loaded with rosuvastatin. *J Liposome Res*. 2018; 28(2):149–160.
53. Hauss DJ, Fogal SE, Ficorilli JV, et al. Lipid-based delivery systems for improving the bioavailability and lymphatic transport of a poorly water-soluble LTB4 inhibitor. *J Pharm Sci*. 1998;87(2):164–169.
54. Kaszuba M, Corbett J, Watson FM, Jones A. High-concentration zeta potential measurements using light-scattering techniques. *Philos Trans A Math Phys Eng Sci*. 2010;368(1927):4439–4451.
55. Khattab A, Hassanin L, Zaki N. Self-Nanoemulsifying Drug Delivery System of Coenzyme (Q10) with Improved Dissolution, Bioavailability, and Protective Efficiency on Liver Fibrosis. *AAPS PharmSciTech*. 2017; 18(5):1657–1672.
56. Oliveira LT, de Paula MA, Roatt BM, et al. Impact of dose and surface features on plasmatic and liver concentrations of biodegradable polymeric nanocapsules. *Eur J Pharm Sci*. 2017;105:19–32.
57. Rambharose S, Kalhapure RS, Govender T. Nanoemulgel using a bicephalous heterolipid as a novel approach to enhance transdermal permeation of tenofovir. *Colloids Surf B Biointerfaces*. 2017;154: 221–227.
58. Honary S, Zahir F. Effect of Zeta Potential on the Properties of Nano-Drug Delivery Systems – A Review (Part 2). *Tropical Journal of Pharmaceutical Research*. 2013;12(2):265–273.
59. Guerra-Rosas MI, Morales-Castro J, Ochoa-Martínez LA, Salvia-Trujillo L, Martín-Belloso O. Long-term stability of food-grade nanoemulsions from high methoxyl pectin containing essential oils. *Food Hydrocolloids*. 2016;52:438–446.
60. Agrawal AK, Aqil F, Jeyabalan J, et al. Milk-derived exosomes for oral delivery of paclitaxel. *Nanomedicine*. 2017;13(5):1627–1636.
61. Mahtab A, Anwar M, Mallick N, Naz Z, Jain GK, Ahmad FJ. Transungual Delivery of Ketoconazole Nanoemulgel for the Effective Management of Onychomycosis. *AAPS PharmSciTech*. 2016;17(6):1477–1490.
62. Teeranachaideekul V, Chantaburanan T, Junyaprasert VB. Influence of state and crystallinity of lipid matrix on physicochemical properties and permeation of capsaicin-loaded lipid nanoparticles for topical delivery. *Journal of Drug Delivery Science and Technology*. 2017; 39:300–307.
63. Dangre P, Gilhotra R, Dhole S. Formulation and statistical optimization of self-microemulsifying drug delivery system of eprosartan mesylate for improvement of oral bioavailability. *Drug Deliv Transl Res*. 2016;6(5):610–621.
64. Nekkanti V, Wang Z, Betageri GV. Pharmacokinetic Evaluation of Improved Oral Bioavailability of Valsartan: Proliposomes Versus Self-Nanoemulsifying Drug Delivery System. *AAPS PharmSciTech*. 2016;17(4):851–862.
65. Caliph SM, Charman WN, Porter CJ. Effect of short-, medium-, and long-chain fatty acid-based vehicles on the absolute oral bioavailability and intestinal lymphatic transport of halofantrine and assessment of mass balance in lymph-cannulated and non-cannulated rats. *J Pharm Sci*. 2000;89(8):1073–1084.
66. Porter CJ, Pouton CW, Cuine JF, Charman WN. Enhancing intestinal drug solubilisation using lipid-based delivery systems. *Adv Drug Deliv Rev*. 2008;60(6):673–691.
67. Seto Y, Kato K, Tsukada R, et al. Protective effects of tranilast on experimental colitis in rats. *Biomed Pharmacother*. 2017;90:842–849.
68. Ivanovska TP, Mladenovska K, Zhivikj Z, et al. Synbiotic loaded chitosan-Ca-alginate microparticles reduces inflammation in the TNBS model of rat colitis. *Int J Pharm*. 2017;527(1–2):126–134.
69. Mi H, Liu FB, Li HW, Hou JT, Li PW. Anti-inflammatory effect of Chang-An-Shuan on TNBS-induced experimental colitis in rats. *BMC Complement Altern Med*. 2017;17(1):315.
70. Jin H, Guo J, Liu J, et al. Anti-inflammatory effects and mechanisms of vagal nerve stimulation combined with electroacupuncture in a rodent model of TNBS-induced colitis. *Am J Physiol Gastrointest Liver Physiol*. 2017;313(3):G192–G202.
71. Wang H, Gu J, Hou X, et al. Anti-inflammatory effect of miltirone on inflammatory bowel disease via TLR4/NF-κB/IQGAP2 signaling pathway. *Biomed Pharmacother*. 2017;85:531–540.
72. Umehara Y, Kudo M, Nakaoka R, Kawasaki T, Shiomi M. Serum proinflammatory cytokines and adhesion molecules in ulcerative colitis. *Hepatogastroenterology*. 2006;53(72):879–882.
73. Biagioli M, Laghi L, Carino A, et al. Metabolic Variability of a Multispecies Probiotic Preparation Impacts on the Anti-inflammatory Activity. *Front Pharmacol*. 2017;8:505.
74. Fiocchi C. Inflammatory bowel disease: etiology and pathogenesis. *Gastroenterology*. 1998;115(1):182–205.
75. Zarzecki MS, Bortolotto VC, Poetini MR, et al. Anti-Inflammatory and Anti-Oxidant Effects of p-Chloro-phenyl-selenoesterol on TNBS-Induced Inflammatory Bowel Disease in Mice. *J Cell Biochem*. 2017;118(4):709–717.
76. Gong XP, Sun YY, Chen W, et al. Anti-diarrheal and anti-inflammatory activities of aqueous extract of the aerial part of Rubia cordifolia. *BMC Complement Altern Med*. 2017;17(1):20.
77. Zhao J, Hong T, Dong M, Meng Y, Mu J. Protective effect of myricetin in dextran sulphate sodium-induced murine ulcerative colitis. *Mol Med Rep*. 2013;7(2):565–570.
78. Mandalari G, Bisignano C, Genovese T, et al. Natural almond skin reduced oxidative stress and inflammation in an experimental model of inflammatory bowel disease. *Int Immunopharmacol*. 2011;11(8): 915–924.
79. Szandruk M, Merwid-Ląd A, Szeląg A. The impact of mangiferin from Belamcanda chinensis on experimental colitis in rats. *Inflammopharmacology*. 2018;26(2):571–581.
80. Wei W, Feng W, Xin G, Wu W, Wang F, Gao X, et al. Enhanced effect of κ-carrageenan on TNBS-induced inflammation in mice. *Int Immunopharmacol*. 2016;39:218–228.
81. Akanda MR, Nam HH, Tian W, Islam A, Choo BK, Park BY. Regulation of JAK2/STAT3 and NF-κB signal transduction pathways; Veronica polita alleviates dextran sulfate sodium-induced murine colitis. *Biomed Pharmacother*. 2018;100:296–303.
82. Barker EC, Kim BG, Yoon JH, Tochtrop GP, Letterio JJ, Choi SH. Potent suppression of both spontaneous and carcinogen-induced colitis-associated colorectal cancer in mice by dietary celastrol supplementation. *Carcinogenesis*. 2018;39(1):36–46.
83. Pan MH, Hsieh MC, Hsu PC, et al. 6-Shogaol suppressed lipopolysaccharide-induced up-expression of iNOS and COX-2 in murine macrophages. *Mol Nutr Food Res*. 2008;52(12):1467–1477.
84. Akira S, Takeda K. Toll-like receptor signalling. *Nat Rev Immunol*. 2004;4(7):499–511.
85. Siddique I, Khan I. Mechanism of regulation of Na-H exchanger in inflammatory bowel disease: role of TLR-4 signaling mechanism. *Dig Dis Sci*. 2011;56(6):1656–1662.

Supplementary materials

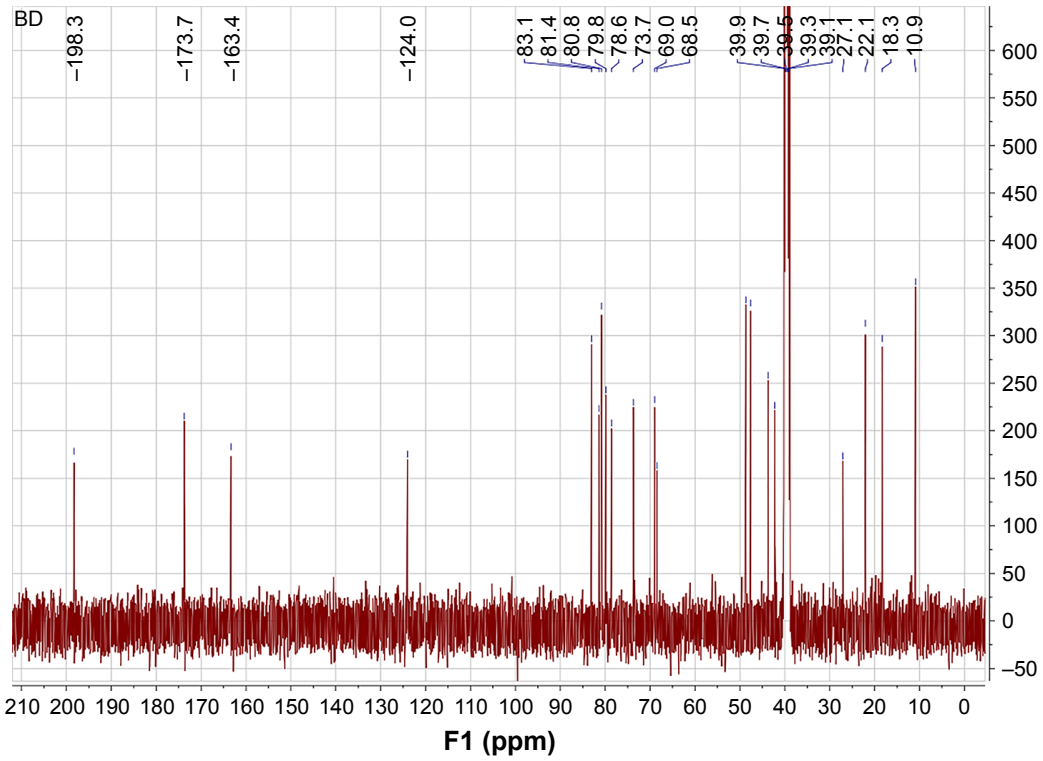

Figure S1 ^{1}H-NMR spectrum of bruceine D.

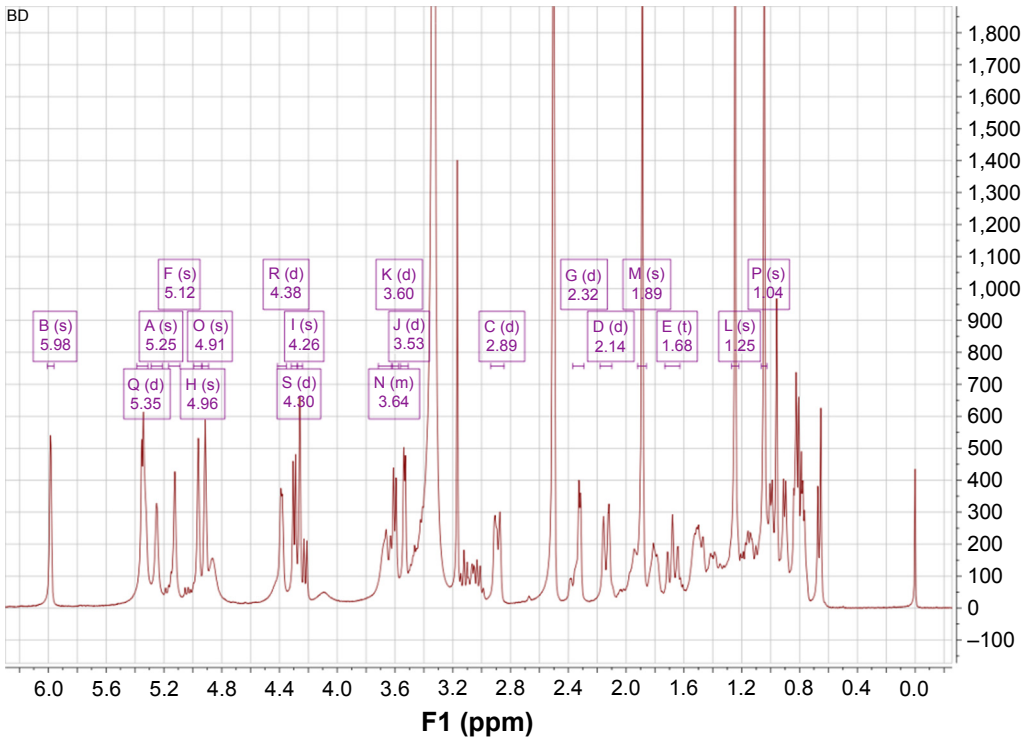

Figure S2 ^{13}C-NMR spectrum of bruceine D.